PROBABILITY DISTRIBUTION OF CW INDUCED CURRENTS ON RANDOMLY ORIENTED SUB-RESONANT LOOPS AND WIRES

R & D Associates
4640 Admiralty Way
Marina del Rey, California 90291 ·

May 1976

Topical Report

CONTRACT No. DNA 001-76-C-0001

APPROVED FOR PUBLIC RELEASE;
DISTRIBUTION UNLIMITED.

Prepared for

Director

DEFENSE NUCLEAR AGENCY

Washington, D. C. 20305

SECURITY CLASSIFICATION OF THIS PAGE *(When Data Entered)*

REPORT DOCUMENTATION PAGE		READ INSTRUCTIONS BEFORE COMPLETING FORM
1. REPORT NUMBER DNA 4162T	2. GOVT ACCESSION NO.	3. RECIPIENT'S CATALOG NUMBER
4. TITLE *(and Subtitle)* PROBABILITY DISTRIBUTION OF CW INDUCED CURRENTS ON RANDOMLY ORIENTED SUB-RESONANT LOOPS AND WIRES		5. TYPE OF REPORT & PERIOD COVERED Topical Report
		6. PERFORMING ORG. REPORT NUMBER
7. AUTHOR(s) William R. Graham Charles T. C. Mo		8. CONTRACT OR GRANT NUMBER(s) DNA 001-76-C-0001
9. PERFORMING ORGANIZATION NAME AND ADDRESS R & D Associates 4640 Admiralty Way Marina del Rey, California 90291		10. PROGRAM ELEMENT, PROJECT, TASK AREA & WORK UNIT NUMBERS Subtask P99QAXDB001-17
11. CONTROLLING OFFICE NAME AND ADDRESS Director Defense Nuclear Agency Washington, D.C. 20305		12. REPORT DATE May 1976
		13. NUMBER OF PAGES 70
14. MONITORING AGENCY NAME & ADDRESS*(if different from Controlling Office)*		15. SECURITY CLASS *(of this report)* UNCLASSIFIED
		15a. DECLASSIFICATION. DOWNGRADING SCHEDULE

16. DISTRIBUTION STATEMENT *(of this Report)*

Approved for public release; distribution unlimited.

17. DISTRIBUTION STATEMENT *(of the abstract entered in Block 20, if different from Report)*

18. SUPPLEMENTARY NOTES

19. KEY WORDS *(Continue on reverse side if necessary and identify by block number)*

EMP Coupling
Statistical Approach
Complicated Systems
Induced Current Probabilities

20. ABSTRACT *(Continue on reverse side if necessary and identify by block number)*

The deterministic prediction of both transient and CW field coupling to large complex electrical systems poses such a formidable problem that other approaches to predicting the coupling may be useful. In this paper, we analyze the continuous wave coupling to a complicated electrical system in terms of random small dipole interactions in the low frequency limit (wavelengths >> system components' sizes). Both random

DD $_{1\ JAN\ 73}^{FORM}$ **1473** EDITION OF 1 NOV 65 IS OBSOLETE

SECURITY CLASSIFICATION OF THIS PAGE *(When Data Entered)*

20. ABSTRACT (Continued)

coupling to the incident wave and random interactions among the dipoles are considered. The variables being randomized are the incident direction and polarization, the sizes and orientations of the dipoles, the mutual coupling strengths, and the lumped load impedances. The resulting normalized current distributions are shown to be insensitive to the details of the model except at the extremely low and high percentiles.

The magnetic dipole case is investigated in detail. Its resulting induced current distribution roughly resembles, but is not, a log-normal distribution with a standard deviation in the vicinity of $\sim$ 6-7 dB. This result provides insight into some recent measurements obtained for EMP transient field coupling to large systems.

An important implication of the results is that for a variety of complicated systems, essentially consisting of many small elements that the coupling is dominated by low frequency magnetic fields, the central parts of the induced current probability distributions are similar and nearly log-normal. However, conclusions based on the extrapolation of log-normality from measured values near the median to the extreme percentiles may be susceptible to sizeable errors.

Presented in the appendices to indicate a larger scope of the statistical approach are the basic results for some simple electric dipole cases and an investigation of the difference in effects caused by an elliptically polarized incident wave versus a linearly polarized one.

PREFACE

The authors wish to express their appreciation to Dr. C. E. Baum for a brief but interesting discussion of the subject addressed in this report.

TABLE OF CONTENTS

LIST OF ILLUSTRATIONS

LIST OF ILLUSTRATIONS (Continued)

LIST OF TABLES

SECTION 1
INTRODUCTION AND SUMMARY

Not only does electromagnetic (EM) coupling to an electronic system take place through intentional penetrations such as antennas and waveguides, but in addition there usually are present many inadvertent EM coupling paths through cables, apertures, grounding loops, etc. While usually designed to handle the normal signal and noise background adequately, an unhardened system subjected to an unusual EM disturbance such as a radiated continuous wave (CW) field or the electromagnetic pulse (EMP) produced by a nuclear detonation may be caused to malfunction by spurious signals introduced through these inadvertent coupling paths. Analyzing and predicting inadvertent coupling for the purpose of assessing and protecting a complex system has historically been and still is a difficult and challenging task.

While in principle an arbitrarily accurate analysis of the EM coupling can be derived by solving the Maxwell equations in the context of a boundary value problem [1], in reality even for a relatively simple system, such a classical deterministic approach often demands more effort and resources than are available. To keep the mathematics tractable, judicious use of approximations and engineering judgments are inevitably required. Even so, the effort presently needed to obtain approximate deterministic predictions for EM coupling to complicated systems is still substantial [2]. On the other hand, when the statistical properties of the coupling by themselves play a dominant role in the problem being addressed, a much less detailed probabilistic approach may be adequate. In view of these observations, a statistical theory like the

7

the one presented in this paper may provide a productive new approach to EM interaction technology.

The problem of describing the EM interaction with the many interaction paths and modes of a system has some similarity to the problem of describing the behavior of a gas in a box. One possible approach to analyzing the gas problem is to work out the interaction forces and then apply Newton's law to solve simultaneously for the dynamics of all the gas molecules --a rigorously correct approach which has met with very limited success. An alternate approach is to take advantage of the fact that there are a large number of degrees of freedom in the motion of the molecules and to formulate a statistical model of the gas [3]. While this statistical approach reveals much less information than the deterministic one and predicts only the statistical properties of the gas, it has nevertheless proven to be of considerable practical value. Similarly, the EM interaction with a complicated system consisting of a large number of similar basic coupling elements can be modeled statistically to yield a number of interesting results. Applications of these results include estimating the distribution of EM coupling data to be obtained for large systems, and interpreting the experimental results.

The fundamental approximation in the probabilistic approach to EM coupling is the hypothesis of a basic element of interaction whose parameters are statistically distributed. We take this basic element of interaction to be the small dipole (although a more complex element could be accommodated by the theory) and the basic variables randomized are the incident polarization and direction, the sizes and orientations of the basic dipoles, the mutual coupling strengths, and the lumped load impedances. The basic elements and variables are

8

then aggregated in a probabilistically rigorous manner to yield the final results. In contrast to the deterministic approach, such probabilistic models, when applicable, do not become proportionally more complicated but should yield increasingly accurate results as systems being analyzed become more complicated, if this complication results from the repetition of the basic element. However, we emphasize that the validity of the probabilistic approach to EM coupling should be reviewed for each case to which it is applied.

For complicated systems when the coupling is dominated by low frequency magnetic fields, a wide range of basic coupling element parameters and statistical distributions produce a current probability distribution whose central part is nearly log-normal with a standard deviation of about 6 to 7 dB. However, conclusions based on the extrapolation of the log-normality of the current distribution from the values near the median to the extreme percentiles are susceptible to substantial errors. These results may provide some insight into similar EMP coupling data to large systems [4] obtained for PREMPT (Program for EMP Testing) [5].

To indicate the scope of the statistical coupling method, an investigation of the basic results for some simple electric dipole cases is also presented, as is the difference in effects caused by the elliptically polarized incident waves and linearly polarized ones. In the following text, Section 2 presents the statistical physical models. Section 3 considers the magnetic dipole interaction case, and shows a comparison with PREMPT experimental data. Section 4 presents results for specific electric dipole cases, while Section 5 investi-

gates the difference in effects as caused by elliptically versus linearly polarized incident waves.

The results obtained for subresonant CW excitation appear to be sufficiently interesting to warrant investigation of the response of resonant electric structures to transient electromagnetic waves.

SECTION 2
STATISTICAL PHYSICAL MODEL

2.1 BASIC MODELS

Consider a plane EM wave, with a linearly polarized magnetic field $\underset{\sim}{H}$ and a frequency ω, incident upon a thin and small circular loop [6], as shown in Figure 1. To obtain a basic statistical model, we randomize both the incident field and the loop configuration to have the random variables (Θ_{in}, Φ_{in}) for the incident wave direction, Ψ for the incident magnetic polarization, (Θ, Φ) for the loop's normal direction $\hat{n}$, and R for the loop's radius. Accordingly, the induced current has an amplitude [7]

$$I = \left| \frac{V}{Z_{loop}} \right| \sim \left| \frac{\sqrt{-1}\omega\mu A_o \underset{\sim}{H} \cdot \hat{n}}{\sqrt{-1}\omega L_w + R_{rad} + R_{loss}} \right| \qquad (1)$$

where μ is the permeability of the surrounding medium (usually its vacuum value μ_o), A_o the loop's area, L_w its inductance, and R_{rad} and R_{loss} respectively its radiation and wire-loss resistance. For a small and thin loop, the induced current random variable I [8], from (1), can be normalized such that the assumed value i is given by

$$i = \eta \frac{r}{r_m} \qquad 0 \leq i \leq 1 \qquad (2)$$

with

$$\eta = |\cos\theta \cos\psi \sin\theta_{in} - \sin\theta [\cos\psi \cos\theta_{in}$$
$$- \cos(\phi - \phi_{in}) + \sin\psi \sin(\phi - \phi_{in})]|. \qquad (3)$$
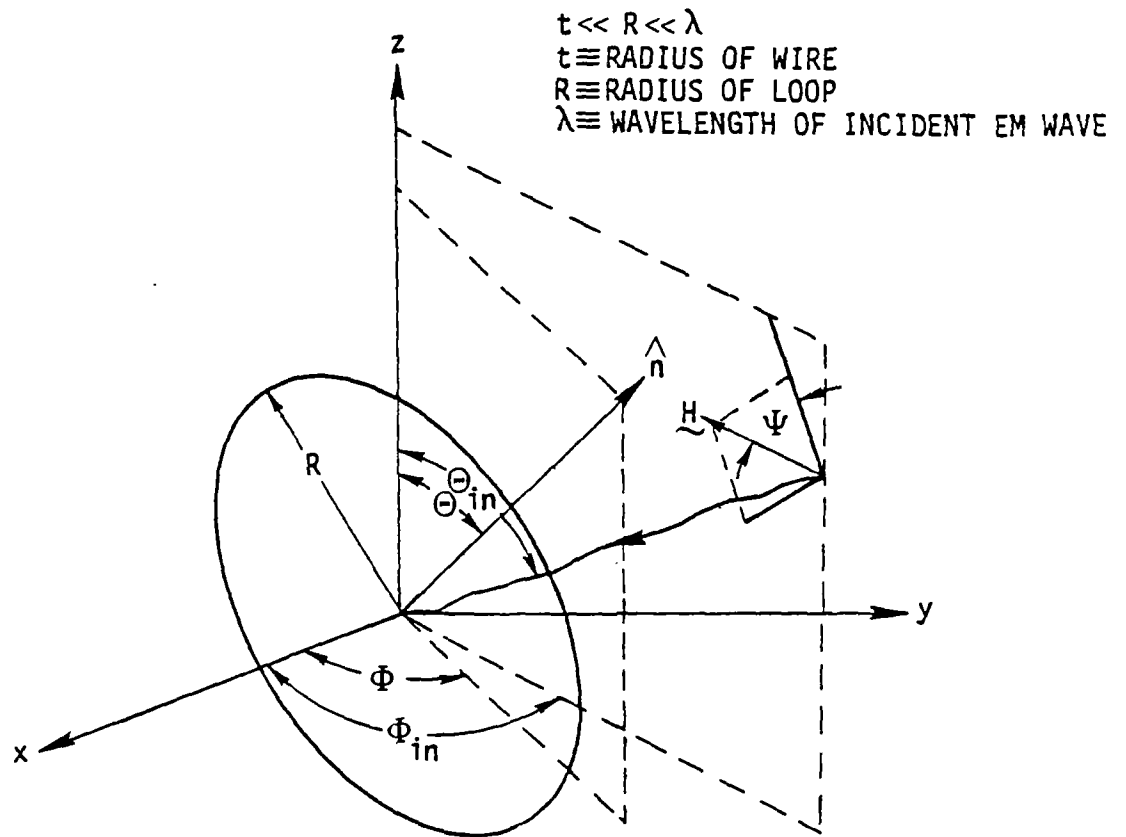
Figure 1. Orientation of the Incident Field
and the Loop with Normal $\hat{n}$

Here, $r \leq r_m$, $0 \leq \theta \leq \pi$, $0 \leq \phi_{in} \leq 2\pi$, $0 \leq \theta_{in} \leq \pi$, $0 \leq \phi_{in} \leq 2\pi$, and $0 \leq \psi \leq 2\pi$ are the values taken respectively by the random variables R, Θ, Φ, Θ_{in}, Φ_{in}, and Ψ with their corresponding probability densities denoted by $p_R(r)$, $p_{\Theta,\Phi}(\theta,\phi)$, $p_{\Theta_{in},\Phi_{in}}(\theta_{in},\phi_{in})$, and $p_\Psi(\psi)$. In terms of these, the normal-ized induced current has a probability distribution

$$F^{(loop)}\{I \leq i\} = \int_{r \leq \frac{ir_m}{\eta}} p_{\Theta,\Phi}(\theta,\phi) \, d\theta d\phi \, p_{\Theta_{in},\Phi_{in}}(\theta_{in},\phi_{in})$$

$$\cdot \, d\theta_{in}d\phi_{in} \, p_\Psi(\psi) \, d\psi \, p_R(r)dr \tag{4}$$

and a probability density

$$p_I^{(loop)}(i) = \frac{d}{di} F^{(loop)}\{I \leq i\}. \tag{5}$$

Equations (2) to (6) give the procedure to compute the probability distribution of the induced current from those of the randomized model parameters.

For the coupling mechanism based on short electric dipoles, as shown in Figure 2, we can model it similarly. For this case, the induced current's amplitude is [9]

$$I \sim \frac{M}{L/2} \cdot \frac{L^2|\underset{\sim}{E} \cdot \hat{L}|}{\ln\left(\frac{L}{D}\right)} \tag{6}$$
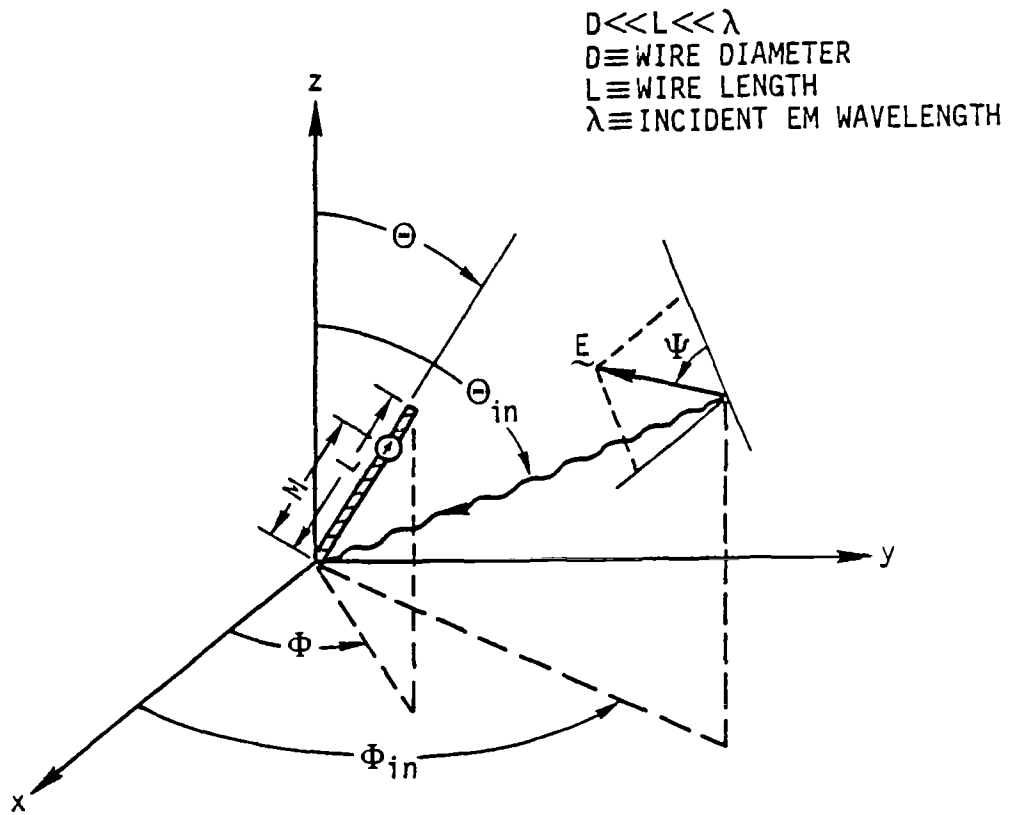
Figure 2. Orientation of the Incident Field and the Wire

where L is the length of the wire with direction unit vector $\hat{L}$, M the position along the wire at which the current is considered, D the diameter of the wire, and $\underset{\sim}{E}$ the incident electric field. Compared with the magnetic coupling case, the differences are that $\underset{\sim}{E}$, $\hat{L}$, and L replace, respectively, $\underset{\sim}{H}$, $\hat{n}$, and R and that the additional random variables M and D are introduced. From Equation 6, the normalized induced current assumes the values

$$i = \frac{\eta s x^2 \ln b}{b^2 \ln x}, \qquad 0 \leq i \leq 1. \tag{7}$$

Here η is given by (3), $0 \leq s \leq 1$ is the value assumed by the random variable $S \equiv M/(L/2)$ with probability density $p_S(s)$, and $1 << x \leq b$ is the value assumed by the dimensionless length $X \equiv L/D$ with density $p_X(x)$ where b is some largest length constant. Finally, from (6) and (7), we have the normalized induced currents' probability distribution

$$F^{(\text{wire})}\{I \leq i\} = \int_{\frac{sx^2\eta}{\ln x} \leq i \frac{b^2}{\ln b}} p_{\Theta,\Phi}(\theta,\phi) \, d\theta d\phi \, p_{\Theta_{in},\Phi_{in}}(\theta_{in},\phi_{in})$$

$$\cdot \, d\theta_{in} d\phi_{in} \, p_\Psi(\psi) \, d\psi \, p_S(s) \, ds \, p_X(x) \, dx \tag{8}$$

and the corresponding density

$$p_I^{(\text{wire})}(i) = \frac{d}{di} F^{(\text{wire})}\{I \leq i\}. \tag{9}$$

15

The above simple coupling models form the basis of our statistical coupling analysis of induced currents. Before specific cases are examined, we shall make several observations. First, the ratio of the current in the magnetic case to that in the electric case is

$$R \equiv \frac{|I_{magnetic}|}{|I_{electric}|} \sim \frac{4R \; \ell n\left(\frac{L}{D}\right)}{\pi L^2 \; \omega\varepsilon} \cdot \frac{H}{E} \; . \tag{10}$$

This, for a plane EM wave with $|E/H| = \sqrt{\mu/\varepsilon}$, reduces to

$$R \sim \frac{4R \; \ell n\left(\frac{L}{D}\right)}{\pi\omega\sqrt{\mu\varepsilon} \; L^2} = \frac{2R \; \lambda\ell n\left(\frac{L}{D}\right)}{\pi^2 L^2} \; . \tag{11}$$

Thus, for <u>small</u> and <u>thin</u> loops and wires of comparable sizes, i.e., $2R \sim L$, $R \sim \lambda\ell n(L/D)/2\pi^2 R) >> 1$, the magnetic coupling is much more important than the electric one. This leads us to place more emphasis on magnetic field coupling.

Second, some very simple probability densities for angular orientations, to be used later, are listed in Table 1 for convenience.

Third, consider an observation that is very simple but useful in interpreting some of the special results. For a random variable $U \equiv f(Y)|cos\Theta|$, where Θ is the angle between a fixed axis and an orientation equally probable in all spatial directions, Y is positive with a probability density $p_Y(y)$, and $f(y) \geq 0$ and is monotonic such that $f^{-1}(y)$ exists. Then the probability density for U

TABLE 1. SIMPLE ANGULAR ORIENTATION DISTRIBUTIONS

Description	$p_{\Theta,\Phi}(\theta,\phi)$
Equally probable in all directions in space	$\dfrac{\sin\theta}{4\pi}$
Equally probable in all directions on a conical $\theta = \theta_0$ surface	$\dfrac{\delta(\theta - \theta_0)}{2\pi}$
Fixed direction at $\theta = \theta_0$, $\phi = \phi_0$	$\delta(\theta - \theta_0)\,\delta(\phi - \phi_0)$

$$p_U(u) = \int_u^\infty p_Y\left(f^{-1}(y)\right)\left[\frac{d}{dy}\,f^{-1}(y)\right]\frac{dy}{y} \qquad (12)$$

implies

$$up_U'(u) = -p_Y\left(f^{-1}(u)\right)\left[\frac{d}{du}\,f^{-1}(u)\right]. \qquad (13)$$

Thus, if $f(y)$ is a monotonically increasing (decreasing)
function of y, the $p_U(u)$ is a monotonically decreasing
(increasing) function of u. One of the simplest examples
[10] is when $f(y) = y$, in which case U is the projected length
onto a fixed axis of a random length whose spatial orientation
is equally probable in all directions. Then, no matter what
probability distribution that random length has, the $p_U(u)$
is a decreasing function of u--the projected length is more
probable to have smaller values than larger values.

17

Fourth, we emphasize that the simple models considered are for electrically small basic coupling elements, loops or wires, with the interactions among these elements neglected. (Such interactions may be neglected, for example, when the elements are placed far apart so their interactions are small.) However, these mutual interactions can be taken into account and moderately change the resulting current distribution in a predictable way, as will be shown in the next section and the special examples.

2.2 RANDOMIZED MUTUAL COUPLINGS AND IMPEDANCE LOADS

Consider first the mutual couplings by examining the current induced on the kth element due to the incident field and the multiple-scattered fields produced by currents at all other elements [11]:

$$I_k = \alpha_k \left| E_o + \sum_{j \neq k} E_j \right| = I_k^{(o)} \left| 1 + G_k' \right|. \tag{14}$$

Here, the superscript "o" stands for the mutual-coupling-neglected current. Now, since the $\sum_{j \neq k} E_j$ is the sum of a large number of fields of fully randomized current elements, the central limit theory applies [12]. Thus $G_k' \to G' \varepsilon N(\mu_G',$ $\sigma_G',)$, a normal distribution with mean μ_G' and standard deviation σ_G'. However, interested only in the relative amplitude of the induced current, we can normalize out the resulting factor $(1 + \mu_G')$ from (14) and get

$$I = I^{(o)} \left| 1 + G \right| \tag{15}$$

where $G \varepsilon N(0, \sigma_G \equiv \sigma_G'/\sqrt{1 + \mu_G'})$. Thus the standard deviation σ_G of G measures the strength of the mutual

coupling, with $\sigma_G \ll 1$ representing very weak and negligible mutual couplings and $\sigma_G \gtrsim 1$ representing strong coupling. The value of σ_G is, of course, determined by the more detailed physics and geometry of the basic interacting elements and cannot be derived from statistics alone. We shall treat it as a parameter.

From (15) and making use of the formula for the product of random variables, we immediately obtain

$$P_I(i) = \int_0^\infty dx \, \frac{P_{I^{(o)}}(x)}{x} \left[P_{G'}\!\left(\frac{i}{x}\right) + P_{G'}\!\left(\frac{-i}{x}\right) \right], \qquad i \geq 0 \tag{16}$$

where $G' \equiv 1 + G \, \varepsilon \, N(1, \sigma_G)$. Thus, the inclusion of the mutual couplings among the basic dipoles gives rise to an extra factor to the induced currents as shown in (15) and changes the current probability density from $P_{I^{(o)}}(i)$ to $P_I(i)$ according to Equation (16). To the mutual-coupling-neglected and normalized current $I^{(o)}$, which distributes itself in the interval $[0,1]$, such an inclusion tends to enhance the probability density for smaller i and to give rise to a prolonged density tail for $i > 1$. For the mean μ_I and the standard deviation σ_I, a simple calculation using (16) shows

$$\mu_I = \mu_{I^{(o)}} \left[\sqrt{\frac{2}{\pi}} \, \sigma_G e^{-1/(2\sigma_G^2)} + 2 \int_0^{1/\sigma_G} \frac{dx}{\sqrt{2\pi}} \, e^{-x^2/2} \right] \tag{17a}$$

$$\xrightarrow{\sigma_G \ll 1} \mu_I(o)\left[1 + O(\sigma_G)\right] \tag{17b}$$

$$\xrightarrow{\sigma_G \gg 1} \mu_I(o) \cdot \sqrt{\frac{2}{\pi}}\,\sigma_G \cdot \left[1 + O\!\left(\frac{1}{\sigma_G}\right)\right] \tag{17c}$$

and

$$\left(\frac{\sigma_I}{\mu_I}\right)^2 = \frac{\left[1 + \left(\frac{\sigma_I(o)}{\mu_I(o)}\right)^2\right]\left[1 + \sigma_G^2\right]}{\left[\sqrt{\frac{2}{\pi}}\,\sigma_G\,e^{-1/(2\sigma_G^2)} + 2\int_0^{1/\sigma_G} \frac{dx\; e^{-1/(2x^2)}}{\sqrt{2\pi}}\right]^2} - 1 \tag{18a}$$

$$\xrightarrow{\sigma_G \ll 1} \left(\frac{\sigma_I(o)}{\mu_I(o)}\right)^2 + O\!\left(\sigma_G^2\right) \tag{18b}$$

$$\xrightarrow{\sigma_G \gg 1} \frac{\pi}{2}\left[1 + \left(\frac{\sigma_I(o)}{\mu_I(o)}\right)^2\right] - 1 + O\!\left(\frac{1}{\sigma_G^2}\right). \tag{18c}$$

Further, one can easily show that the ratio $\left[1 + (\sigma_I/\mu_I)^2\right]/\left[1 + \left(\sigma_I(o)/\mu_I(o)\right)^2\right]$ is monotonically increasing with σ_G.
Thus, this ratio lies between 1 and $\pi/2$ for all σ_G, a variation not too sensitive to the mutual coupling strength σ_G.

Next, consider the effect of a randomized lumped load impedance $R_s + iX_s$ in series with the dipole elements. This renders an induced current

$$I^{(s)} = I^{(o)} \cdot \frac{1}{\sqrt{\left(1 + \frac{X_s}{X_o}\right)^2 + \left(\frac{R_s}{X_o}\right)^2}} \equiv I^{(o)} \cdot F. \qquad (19)$$

where X_o is the dominant reactance of the dipole element. Lacking the detailed information on the distribution of the load impedances, we make the assumption that the probability density associated with an impedance is a decreasing function of the value of the impedance. This is certainly true above some values of impedance, and considering the prevalence of low impedance ground loops in most systems, that value should usually be zero. A simple try would be to have a $p_{1/F}(\xi) = qe^{-q(\xi-1)}$ for $\xi > 1$ and $q > 0$, which includes the case of no load impedance as the parameter $q \to \infty$ and the case of a wide range of virtually uniform loads as $q \to 0$, and consequently results in a $p_F(f) = qe^{+q} f^{-2} e^{-q/f}$ for $0 \leq f \leq 1$. In view of its having a strong zero at $f = 0$ and being a smooth and monotonically increasing function of f in $[0,1]$ but difficult to manipulate mathematically, we can now assume and examine a qualitatively similar but simpler $p_F(f)$ to gain insights into the effects of such a distribution--e.g., by choosing

$$p_F(f) = (n + 1) f^n, \qquad \begin{array}{c} 0 \leq f \leq 1 \\ 0 < n \end{array} \qquad (20)$$

With this $p_F(f)$, we obtain

$$p_{I^{(s)}}(i) = (n + 1) i^n \int_i^\infty dx \cdot \frac{p_{I^{(o)}}(x)}{x^{n+1}} \qquad (21)$$

21

and from which

$$\mu_I(s) = \mu_I(o) \cdot \frac{n+1}{n+2} \tag{22}$$

$$\left(\frac{\sigma_I(s)}{\mu_I(s)}\right)^2 = \left(\frac{\sigma_I(o)}{\mu_I(o)}\right)^2 \cdot \frac{(n+2)^2}{(n+1)(n+3)} + \frac{1}{(n+1)(n+3)} \cdot \tag{23}$$

To effect a strong zero for the $p_F(f \to 0)$ of (20), n must be much greater than 1. Consequently, from (21) to (23), randomized loads have little influence on the induced currents' statistics, except slightly enhancing the near-zero portion of the induced current probability density by $\sim(n+1)/n$ and reducing the value at its end to zero. These results suggest that it may be reasonable to ignore the load impedance random-ization in our special case investigations.

SECTION 3

SPECIAL CASES FOR MAGNETIC LOOPS

In this section we investigate the random coupling results for several cases of the magnetic loop model. This could represent, for example, the EMP coupling with a complicated system consisting of many ground loops. We calculate first the $I^{(o)}$, then take into account mutual coupling by the method outlined in Section 2.2.

3.1 VERTICAL PLANE ORIENTATIONS

Consider first a conductor geometry where nearly all of the loops are in vertical planes, such as might be the case for a single large bay of electrical equipment. If all the loops are in vertical planes, i.e., their normals are horizontal, and have their normal pointed equally probably in all azimuthal directions, then only the horizontal magnetic field component can induce current in the loops and all horizontal field directions have the same effect. Thus, without suffering any loss of generality, we can consider a H_x- polarized plane wave incident along the -z direction (see Figure 1) onto these loops.

Now, if we further assume that the loops' sizes are distributed with equally probable areas between $a_1 = \pi r_1^2$ to $a_2 = \pi r_2^2$, then from (2) to (5) we obtain the probability distribution of the normalized induced current amplitudes

$$F_{(A,2d)}^{(loop)} \left\{ I^{(o)} \leq 1 \right\} = \frac{4}{\pi \left(r_2^2 - r_1^2 \right)} \int_\Omega r \, dr \, d\phi \qquad (24)$$

23

$$\Omega: \begin{cases} r\varepsilon[r_1,r_2] \\ \phi\varepsilon[0,2\pi] \\ r\cos\phi \le i\ r_2 \end{cases}$$

Here, the subscript (A,2d) indicates the case of equally probable areas of loops in two-dimensions. The probability density, from (24), is (see Figure 3)

$$p_{I^{(o)}(A,2d)}^{(loop)}(i) = \frac{4}{\pi(1-\alpha^2)} \begin{cases} \sqrt{1-i^2} - \sqrt{\alpha^2-i^2}, & 0 \le i \le \alpha \\ \sqrt{1-i^2}, & \alpha \le i \le 1 \end{cases}$$

(25)

where $\alpha \equiv r_1/r_2 \le 1$ is the parameter showing the range of spread of the loops' sizes. Thus, the induced normalized current $I^{(o)}$ has a most probable value α, an average

$$\mu_{(A,2d)}^{(o)} = \frac{4(1+\alpha+\alpha^2)}{3\pi(1+\alpha)}$$

(26)

and a standard deviation

$$\sigma_{(A,2d)}^{(o)} = \left\{ \frac{1+\alpha^2}{4} - \left[\frac{4(1+\alpha+\alpha^2)}{3\pi(1+\alpha)}\right]^2 \right\}^{1/2}.$$

(27)

If we assume the loops have equally probable radii, instead of areas, between r_1 and r_2, we then similarly obtain (see Figure 3)

$p_{I^{(0)}}^{(i)}$

$\dfrac{-2\ln a}{\pi(1-a)}$

$\dfrac{4}{\pi(1+a)}$

$\dfrac{2\ln\left(\dfrac{1+\sqrt{1-a^2}}{a}\right)}{\pi(1-a)}$

$\dfrac{4}{\pi\sqrt{1-a^2}}$

$p_{I^{(0)}(A,2d)}^{(loop)}(i)$

$p_{I^{(0)}(R,2d)}^{(loop)}(i)$

$a = \dfrac{r_1}{r_2}$

i

1
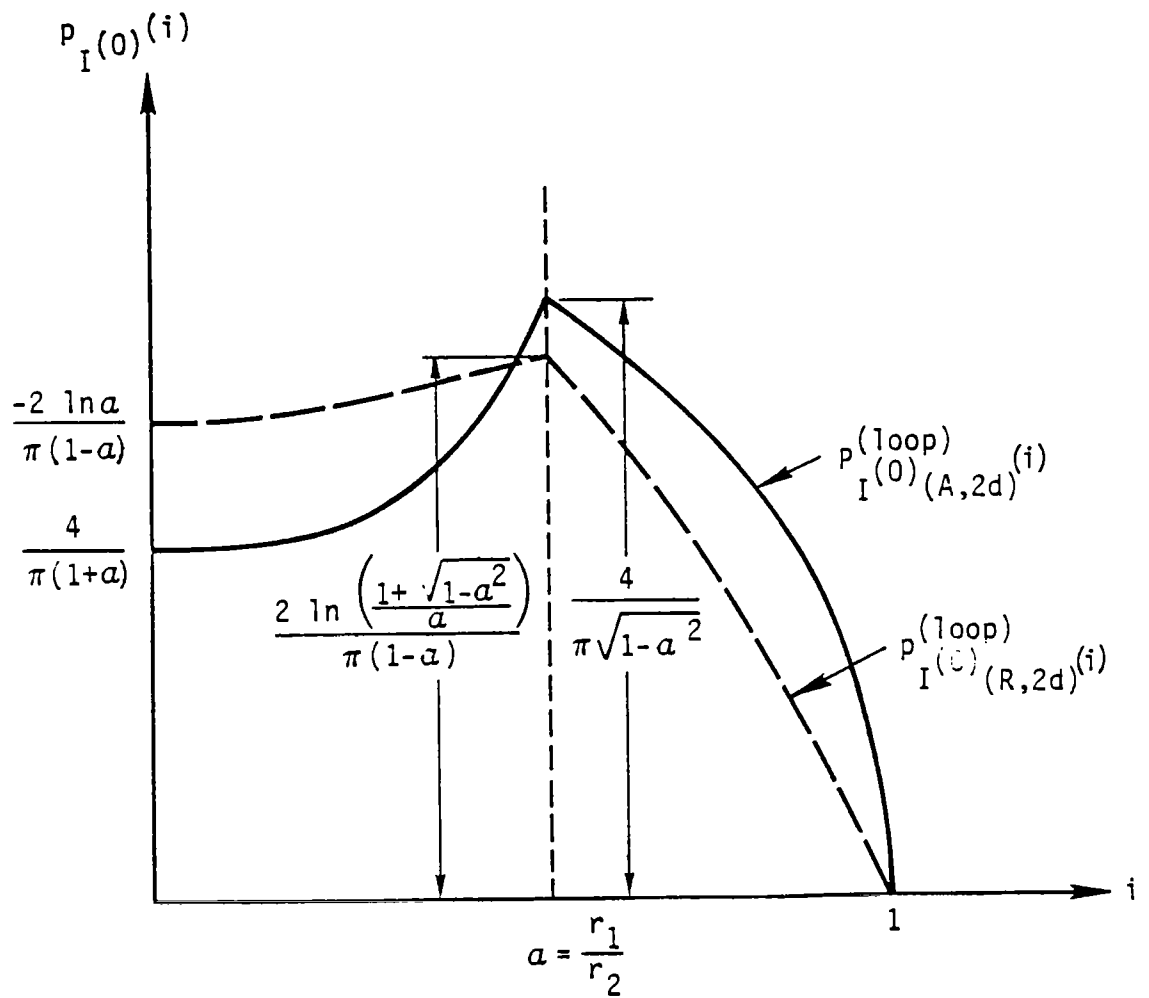
NOTE: $p_{I^{(0)}(R,2d)}^{(loop)}(0) \geqslant p_{I^{(0)}(A,2d)}^{(loop)}(0)$ FOR ALL a

Figure 3. Sketches of $p_{I^{(0)}(A,2d)}^{(loop)}(i)$ and $p_{I^{(0)}(R,2d)}^{(loop)}(i)$, the Normalized Incident Current Probability Densities for Equally Probable Areas and Radii Cases, as Functions of i

$$P_{I^{(o)}(R,2d)}^{(loop)}(i) = \frac{2}{\pi(1-\alpha)} \begin{cases} \ln\left[\dfrac{1+\sqrt{1-i^2}}{\alpha+\sqrt{\alpha^2-i^2}}\right], & 0 \le i \le \alpha \\[4mm] \ln\left[\dfrac{1+\sqrt{1-i^2}}{i}\right], & \alpha \le i \le 1 \end{cases}$$

$$\tag{28}$$

where the subscript $(R,2d)$ indicates the case of equally probable radii in two-dimensions. Its average and standard deviation are [13]

$$\mu_{(R,2d)}^{(o)} = \frac{1+\alpha}{\pi} \tag{29}$$

$$\sigma_{(R,2d)}^{(o)} = \left\{\frac{1+\alpha+\alpha^2}{6} - \left[\frac{1+\alpha}{\pi}\right]^2\right\}^{1/2}. \tag{30}$$

Notice the inequalities $\mu_{(R,2d)}^{(o)} \le \mu_{(A,2d)}^{(o)}$ and $\sigma_{(R,2d)}^{(o)} \le \sigma_{(A,2d)}^{(o)}$, an intuitively plausible result because the equal-probable-area case gives less weight to small sizes than does the equal-probable-radius case. Also, (25) and (28) approach the same expression $2/\left(\pi\sqrt{1-i^2}\right)$ when $\alpha \to 1$, as they should.

The α dependences of the averages and the standard deviations, as well as their ratios, are shown in Table 2. We see that the standard deviations, at about 0.3, are very insensitive to the range of the spread of x (whether a wide spread over 0 to πr_2^2 or a narrow one clustered near πr_2^2) and the nature of the spread (whether equally probable in area or in radius). Also quite so insensitive are the ratios of

26

TABLE 2. AVERAGES AND STANDARD DEVIATIONS FOR MAGNETIC LOOPS EQUALLY
PROBABLY ORIENTED IN VERTICAL PLANES WITHOUT MUTUAL COUPLING

$\alpha \equiv \dfrac{r_1}{r_2}$	$\mu_{(A,2d)}^{(o)}$	$\sigma_{(A,2d)}^{(o)}$	$\dfrac{\sigma_{(A,2d)}^{(o)}}{\mu_{(A,2d)}^{(o)}}$	$\mu_{(R,2d)}^{(o)}$	$\sigma_{(R,2d)}^{(o)}$	$\dfrac{\sigma_{(R,2d)}^{(o)}}{\mu_{(R,2d)}^{(o)}}$
0.0	0.424	0.264	0.623	0.318	0.256	0.803
0.050	0.425	0.264	0.620	0.334	0.252	0.755
0.100	0.428	0.263	0.614	0.350	0.250	0.713
0.150	0.433	0.262	0.604	0.366	0.248	0.677
0.200	0.439	0.260	0.593	0.382	0.247	0.645
0.250	0.446	0.259	0.581	0.398	0.246	0.618
0.300	0.454	0.258	0.559	0.414	0.246	0.594
0.350	0.463	0.258	0.556	0.430	0.246	0.574
0.400	0.473	0.258	0.545	0.446	0.248	0.556
0.450	0.484	0.258	0.534	0.462	0.250	0.541
0.500	0.495	0.260	0.524	0.477	0.252	0.529
0.550	0.507	0.261	0.515	0.493	0.256	0.518
0.600	0.520	0.264	0.508	0.509	0.259	0.509
0.650	0.533	0.267	0.501	0.525	0.264	0.502
0.700	0.547	0.271	0.496	0.541	0.269	0.497
0.707	0.549	0.272	0.495	0.543	0.269	0.496
0.750	0.561	0.276	0.492	0.557	0.274	0.492
0.800	0.575	0.281	0.489	0.573	0.280	0.489
0.850	0.590	0.287	0.486	0.589	0.286	0.486
0.900	0.605	0.293	0.485	0.605	0.293	0.485
0.950	0.621	0.300	0.484	0.621	0.300	0.484
1.000	0.637	0.308	0.483	0.637	0.308	0.483

27

the standard deviations to the corresponding averages, varying from about 0.5 to 0.7.

To correspond to customary electrical engineering practice, we now examine the probability law of $I^{(o)}$ when represented as the (cumulative) probability distribution of its logarithmic value in decibels: $Y^{(o)} \equiv 20 \log_{10} I^{(o)}$. To represent the results, we use a log-normal graph (a log-normal distribution [14] is a positively-sloped straight line in such a graph) to plot the probability distributions $F\{I^{(0)} \leq i\}$ [15]. These plots for the $\alpha = 0$ and $\alpha = 1$ cases are shown in Figure 4. These plots, specified by (25) and (28), are not log-normal and therefore are not straight lines. But they are approximately linear, up to ~75 percent in the (R,2d) and ~60 percent in the (A,2d) cases for $\alpha = 0$ and up to ~50 percent in both cases for $\alpha = 1$; and they flatten to one at higher percentiles. The flattening at the higher percentiles is caused by the induced current being bounded by the maximum response of the basic element of interaction (when mutual coupling is ignored), which provides the normalization of the curves. The effect of the mutual interactions tends to straighten the curves, as was explained by (16) and its following reasoning, and is shown in Figure 5. Figure 5 plots the mutual coupling included distributions $F\{I \equiv I^{(o)} \cdot |1 + G|$ $\leq i\}$, with mutual coupling strengths $\sigma_G = 1$ and $\sigma_G = 30$, for the corresponding cases in Figure 4. Excluding the extreme percentiles, curves in Figure 5 clearly exhibit rather close resemblances to straight lines. The resemblance is better for larger σ_G.

Within this resemblance, I is approximately log-normal and its average μ and standard deviation σ are related approximately to those of $Y \equiv 20 \log_{10} I$ by

Figure 4. Probability Distribution of the Normalized Induced Loop
Currents $I^{(0)}$ for the Two-Dimensional Cases of Equally
Probable Area (A,2d) and Equally Probable Radius (R,2d),
with Size Parameter $\alpha =0$, and $\alpha =1$

Figure 5(a). Probability Distributions of the Induced Loop Currents I
for the Two-Dimensional Case of Equally Probable Area
(A,2d) and Equally Probable Radius (R,2d) with Size
Parameter α =1 and Mutual Coupling Strength σ_G=1 and σ_G=30

30
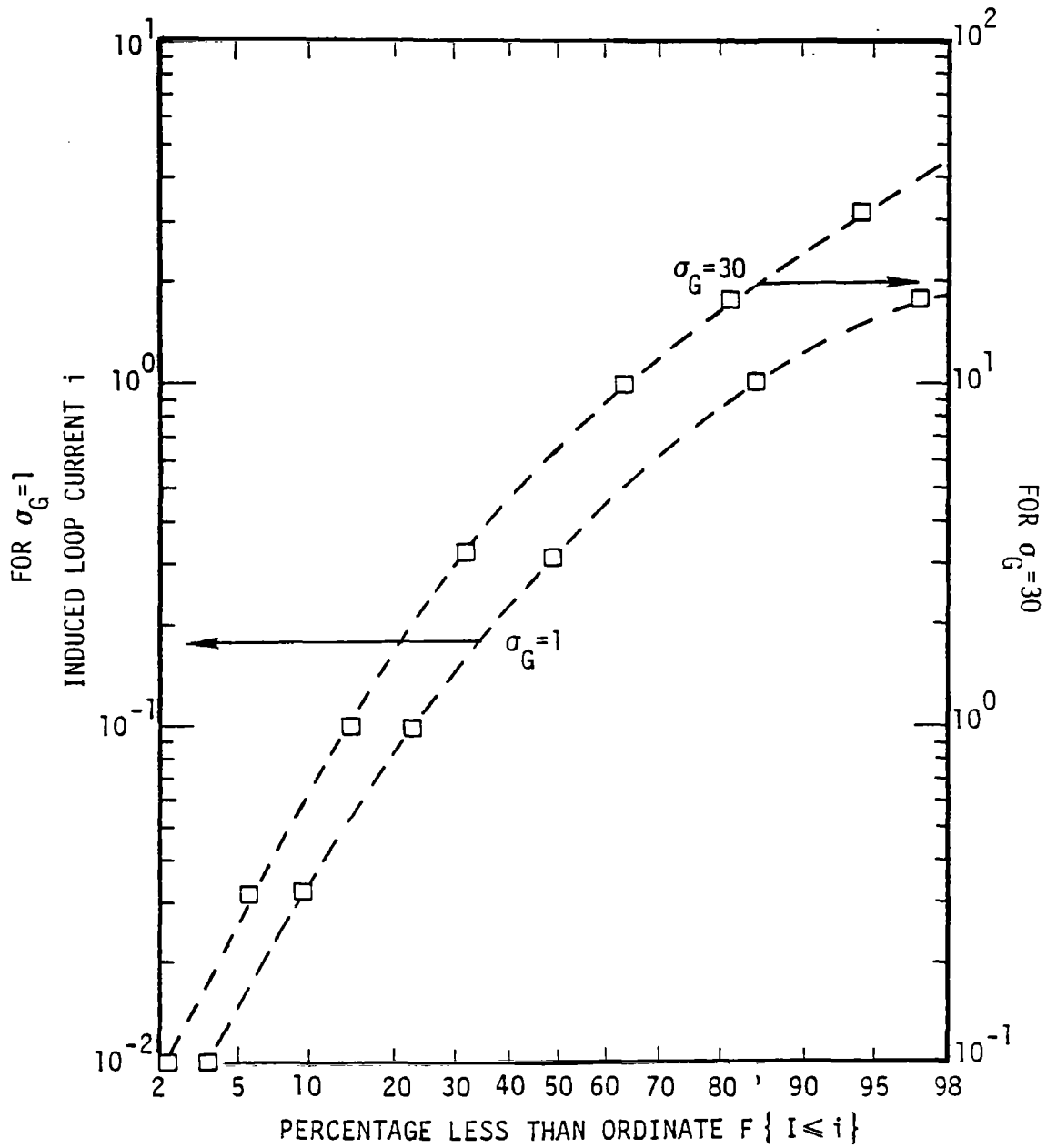
Figure 5(b). Probability Distributions of the Induced Loop Currents I
for the Two Dimensional Case of Equally Probable Area
(A,2d) with Size Parameter $\alpha = 0$ and Mutual Coupling
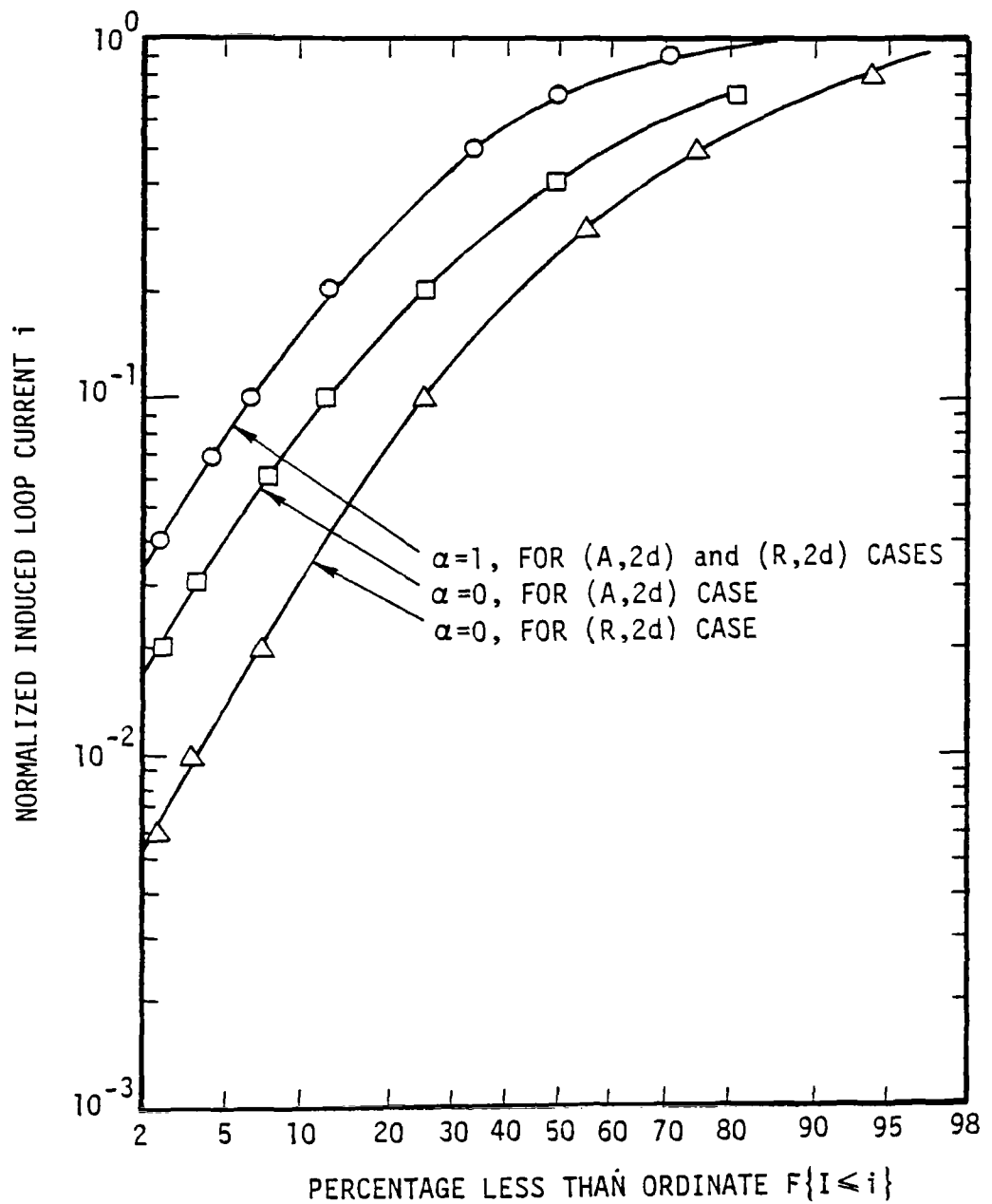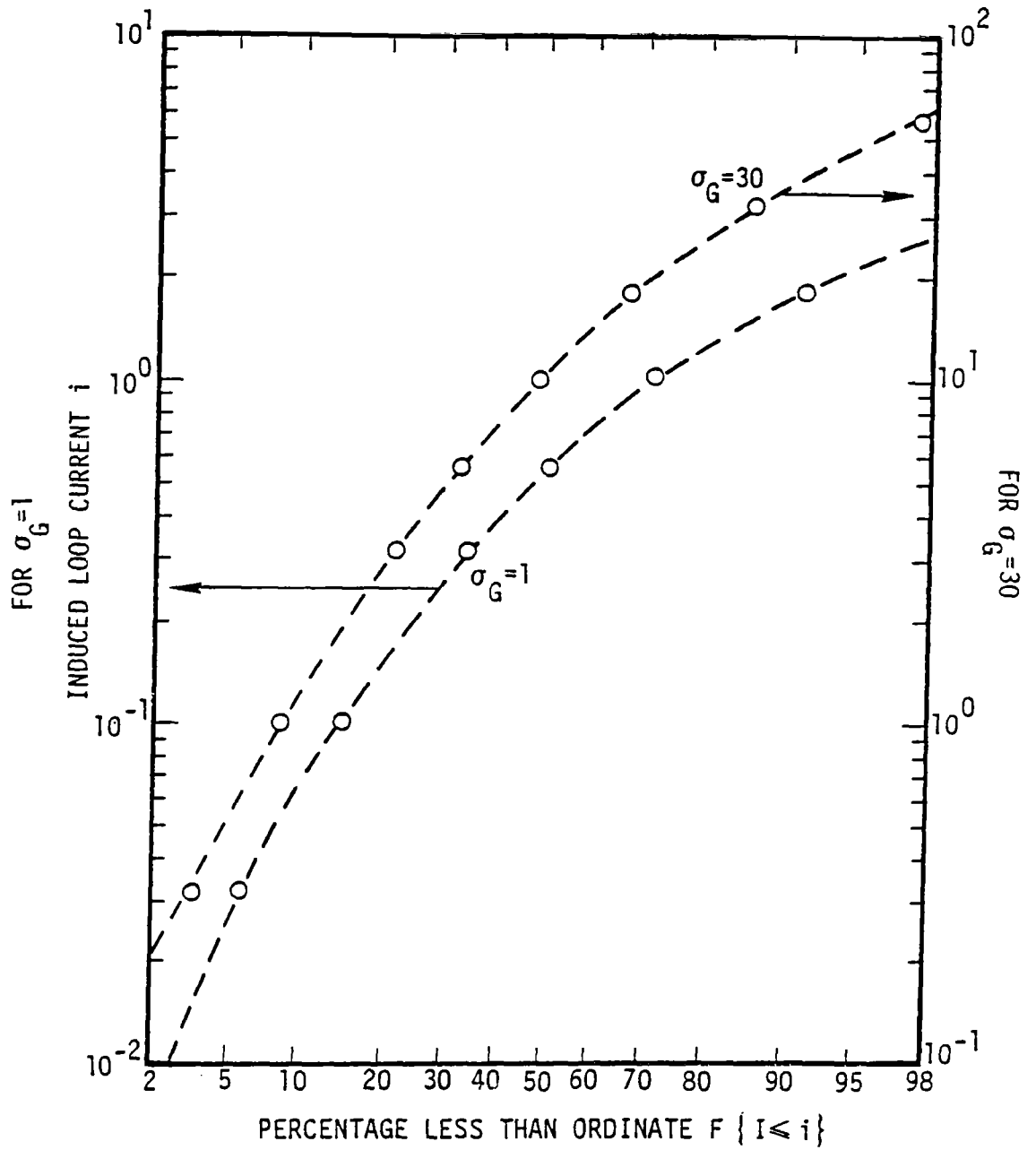Strengths $\sigma_G = 1$ and $\sigma_G = 30$

31
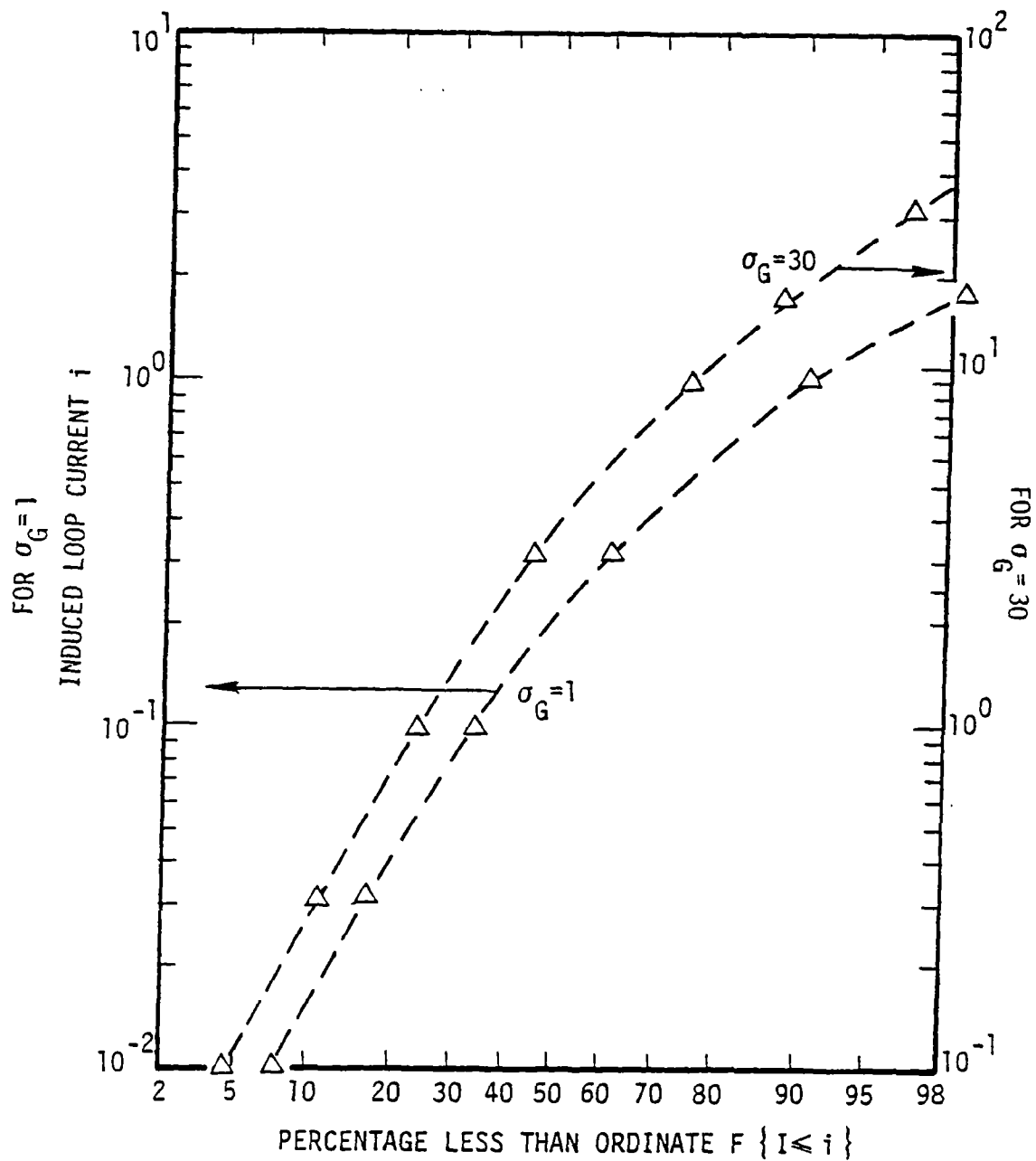
Figure 5(c). Probability Distributions of the Induced Loop Currents I
for the Two-Dimensional Case of Equally Probable Radius
(R,2d) with Size Parameter $\alpha=0$ and Mutual Coupling
Strengths $\sigma_G=1$ and $\sigma_G=30$

$$\mu_Y = \frac{20}{\ln 10} \left\{ \ln \mu - \frac{1}{2} \ln \left[1 + \left(\frac{\sigma}{\mu} \right)^2 \right] \right\} \qquad (31)$$

$$\sigma_Y = \frac{20}{\ln 10} \sqrt{\ln \left[1 + \left(\frac{\sigma}{\mu} \right)^2 \right]} . \qquad (32)$$

Using the relation (18) that links the σ/μ of I to the $\sigma^{(o)}/\mu^{(o)}$ of $I^{(o)}$, we immediately have

$$\sigma_{Y^{(o)}} \leq \sigma_Y \leq \sigma_{Y^{(\infty)}} \qquad (33a)$$

where

$$\sigma_{Y^{(o)}} \equiv \frac{20}{\ln 10} \sqrt{\ln \left[1 + \left(\frac{\sigma^{(0)}}{\mu^{(0)}} \right)^2 \right]} \qquad (33b)$$

$$\sigma_{Y^{(\infty)}} \equiv \frac{20}{\ln 10} \sqrt{\ln \left[\frac{\pi}{2} \left(1 + \left(\frac{\sigma^{(0)}}{\mu^{(0)}} \right)^2 \right) \right]} . \qquad (33c)$$

The superscripts o and ∞ of Y represent, respectively, the cases of $\sigma_G \to 0$ and $\sigma_G \to \infty$. The two limiting standard deviations of the logarithmic currents, $\sigma_{Y^{(o)}}$ and $\sigma_{Y^{(\infty)}}$, are plotted in Figure 6 as functions of $\sigma^{(o)}/\mu^{(o)}$. The shaded area, representing the range of $\sigma^{(o)}/\mu^{(o)}$ given in Table 2, exhibits the narrow range of possible values for the corresponding log-normally distributed standard deviations $\sigma_{Y^{(o)}}$ and $\sigma_{Y^{(\infty)}}$. Figure 6 shows a range of standard deviations for Y encompassing ~ 4 to ~ 8 dB for any distribution-size parameter α, and centered around ~ 6 to ~ 7 dB.
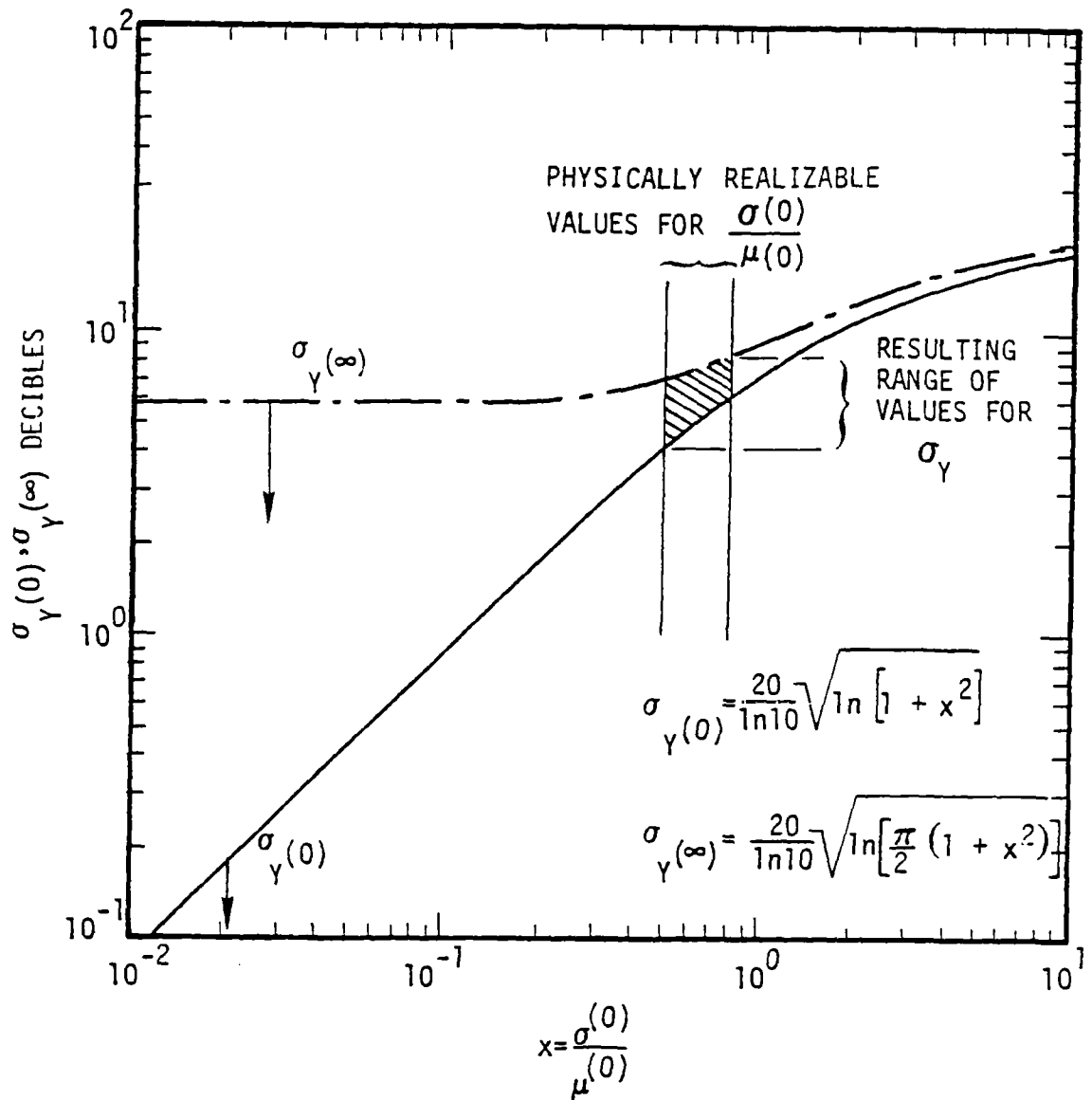
Figure 6. The Limiting Standard Deviations $\sigma_{\gamma}(0)$ and $\sigma_{\gamma}(\infty)$, for 0 and ∞ Mutual Coupling Strengths, of the Logrithmic Currents as Functions of $\sigma^{(0)}/\mu^{(0)}$

34

Very little statistical data on EM coupling to large systems is available, most that exists was taken from the PREMPT program [16]. These tests measured the maximum peak-to-peak current response to broadband pulsed fields and therefore are the result of a more complex interaction than the CW case analyzed in this paper; however, it is still interesting to see if the analysis and the data follow the same general trends.

The distributions of three sets of such measured data, normalized by each of their own median value, are shown in Figure 7 [17]. They are rather similar to each other and are approximately log-normal with standard deviations to their logarithmic values at ∿5 to ∿7 dB. A comparison to the theory and the data is also shown in Figure 7 by overlaying the median-value-normalized theoretical results, for the cases of (A,2d) and (R,2d) with parameters α and σ_G being 0 and 1, on top of the data. The comparison shows rather good agreement for the ∿40 percent and higher percentiles, but displays a discrepancy at low percentiles: there are fewer low (compared with the median value) currents in the data than in the theory. This discrepancy is not surprising. We suspect that the smaller number of low current measurements is caused at least in part by a systematic bias in the current data that would result from an engineering judgment to avoid measuring currents that are obviously uninteresting because they are so small and are difficult to measure in the background of system noise.

To the extent that the theoretical curves can be approximated by straight lines near the median value of the distributions, and therefore by log-normal distributions over this region, the standard deviations implied by their slopes are similar to those of the data (see Figure 6).

35
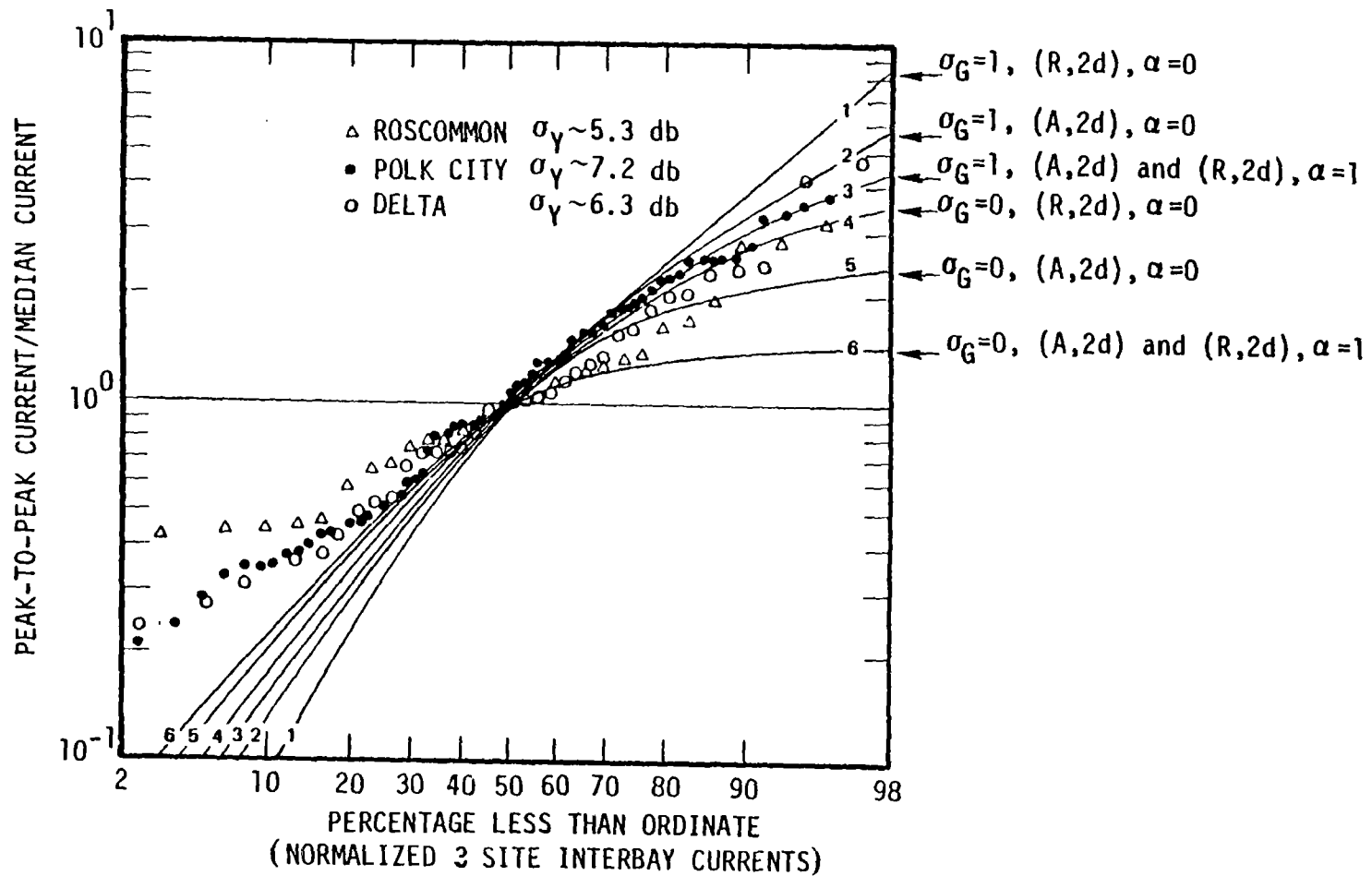
Figure 7. Peak-to-Peak Induced Current Distribution Data for EMP Simulations Obtained in the Program PREMPT and Overlay of 2-D Results

36

3.2 THREE-DIMENSIONAL ORIENTATIONS

For loops oriented equally probable in the three-dimensional space, as might roughly be the case for a large electrical facility, we can obtain the induced current probability densities by the same procedures used in Section 3.1. For the equally probable area case,

$$p_{I^{(o)}(A,3d)}^{(loop)}(i) = \frac{2}{1-\alpha^2} \cdot \begin{cases} 1 - \alpha, & 0 \le i \le \alpha \\ 1 - i, & \alpha \le i \le 1 \end{cases} \tag{34}$$

and

$$\mu_{(A,3d)}^{(o)} = \frac{1 + \alpha + \alpha^2}{3(1 + \alpha)} < \mu_{(A,2d)}^{(o)} \tag{35}$$

$$\sigma_{(A,3d)}^{(o)} = \left[\frac{1 + \alpha^2}{6} - \left(\frac{1 + \alpha + \alpha^2}{3(1 + \alpha)} \right)^2 \right]^{1/2} < \sigma_{(A,2d)}^{(o)}. \tag{36}$$

For the equally probable radius case,

$$p_{I^{(o)}(R,3d)}^{(loop)}(i) = \frac{1}{1-\alpha} \begin{cases} \ln \frac{1}{\alpha}, & 0 \le i \le \alpha \\ \ln \frac{1}{i}, & \alpha \le i \le 1 \end{cases} \tag{37}$$

and

$$\mu_{(R,3d)}^{(o)} = \frac{1 + \alpha}{4} < \mu_{(R,2d)}^{(o)} \tag{38}$$

37

$$\sigma^{(o)}_{(R,3d)} = \left[\frac{1 + \alpha + \alpha^2}{9} - \left(\frac{1 + \alpha}{4} \right)^2 \right]^{1/2} < \sigma^{(o)}_{(R,2d)} . \qquad (39)$$

The three-dimensional probability densities are depicted in Figure 8. They are monotonically decreasing functions of i, as expected in view of the remark made at (12) and (13). Also, they favor lower current values more than their two-dimensional counterparts do, as can be seen easily in Figure 8 or by observing the inequalities in (35) to (39). Such a behavior is intuitively obvious because in three-dimensions, unlike in two-dimensions, there is more solid angle within a $\Delta\theta$ near the perpendicular to a given direction than there is near the parallel. Furthermore, similar to the two-dimensional cases, we have $\mu^{(o)}_{(R,3d)} \leq \mu^{(o)}_{(A,3d)}$ and $\sigma^{(o)}_{(R,3d)} \leq \sigma^{(o)}_{(A,3d)}$. Table 3 lists the numerical dependences on α of the averages and standard deviations. They exhibit even more insensitivity to the changes in α than the two-dimensional cases do. Figure 9, similar to Figure 4, plots in log-normal graphs the distribution of $I^{(o)}$ for the three-dimensional cases (A,3d) and (R,3d) with $\alpha = 0$ and $\alpha = 1$. Finally, we point out that an inclusion of the mutual coupling effect, similar to that in Section 3.1, again renders a cumulative current distribution that is in its central part roughly log-normal and results in standard deviations for 20 $\log_{10}$ I even slightly more closely packed near ~ 6 dB. The last statement can be easily seen by reading the $\sigma^{(o)}/\mu^{(o)}$ values of Table 3 into Figure 6. A comparison of the PREMPT data and the three-dimensional loop distribution results, similar to the two-dimensional results shown in Figure 7, is shown in Figure 10. As before, the trends in the theory and the data correspond quite well.

```
 .00000    .00000    .00000    .00000    .00000    .00000    .00000    .00000    .00000    .00000
 .00000    .00000    .00000    .00000    .00000    .00000    .00000    .00000    .00000    .00000
 .11000    .09625    .08250    .06875    .05500    .04125    .02750    .01375    .00000    .00000
 .00000    .00000    .00000    .00000    .00000    .00000    .00000    .00000    .00000    .00000
-.01375  -.02750  -.22000  -.20625  -.19250  -.17875  -.16500  -.15125  -.13750  -.12375
-.11000  -.09625  -.08250  -.06875  -.05500  -.04125  -.02750  -.01375    .00000    .00000
 .00000    .00000    .00000    .00000    .00000    .00000    .00000    .00000    .00000    .00000
   1  12  23  42
   1   9  19  37
+0.0022200E+00+0.0011100E+00+0.0022200E+00+0.0011100E+00
   0
   3
  90.    90.-0.100000E+01+0.000000E+00+0.000000E+00+0.000000E+00
  60.    90.-0.100000E+01+0.000000E+00+0.000000E+00+0.000000E+00
  30.    90.-0.100000E+01+0.000000E+00+0.000000E+00+0.000000E+00
```

Output

```
NW  NP  NR     BK
 4  50   4  0.6283184E 01

PX
  0.0       0.0       0.0       0.0       0.0       0.0       0.0       0.0
  0.0       0.0137    0.0275    0.1100    0.0962    0.0825    0.0687    0.0550
  0.0412    0.0275    0.0137    0.0       0.0       0.0       0.0       0.0
  0.0       0.0       0.0       0.0       0.0       0.0       0.0       0.0
  0.0       0.0       0.0       0.0       0.0       0.0       0.0      -0.0137
 -0.0275   -0.1100   -0.0962   -0.0825   -0.0687   -0.0550   -0.0412   -0.0275
 -0.0137    0.0

PY
  0.0       0.0       0.0       0.0       0.0       0.0       0.0       0.0
  0.0       0.0       0.0       0.0       0.0       0.0       0.0       0.0
  0.0       0.0       0.0       0.0       0.0       0.0       0.0       0.0
  0.0       0.0       0.0       0.0       0.0       0.0       0.0       0.0
  0.0       0.0       0.0       0.0       0.0       0.0       0.0       0.0
  0.0       0.0       0.0       0.0       0.0       0.0       0.0       0.0
  0.0       0.0

PZ
  0.1100    0.0962    0.0825    0.0687    0.0550    0.0412    0.0275    0.0137
  0.0       0.0       0.0       0.0       0.0       0.0       0.0       0.0
  0.0       0.0       0.0       0.0      -0.0137   -0.0275   -0.2200   -0.2062

 -0.1925   -0.1787   -0.1650   -0.1512   -0.1375   -0.1237   -0.1100   -0.0962
 -0.0825   -0.0687   -0.0550   -0.0412   -0.0275   -0.0137    0.0       0.0
  0.0       0.0       0.0       0.0       0.0       0.0       0.0
  0.0       0.0
```

```
LL
   1   12   23   42

LR
   1    9   19   37

RAD
 0.2220000E-02 0.1110000E-02 0.2220000E-02 0.1110000E-02

NSET
  3


********

THETA    PHI           EI(1)                    EI(2)
  90.    90.-0.1000E 01 0.0          0.0          0.0

CURRENT
   I      REAL          IMAG          MAGNITUDE      PHASE
   1  -0.501472E-04 -0.266968E-03  0.271637E-03   -100.621
   2  -0.820176E-04 -0.435063E-03  0.442726E-03   -100.659
   3  -0.105347E-03 -0.557393E-03  0.567261E-03   -100.685
   4  -0.116468E-03 -0.615480E-03  0.626403E-03   -100.698
   5  -0.226121E-04 -0.115846E-03  0.118032E-03   -101.027
   6  -0.388146E-04 -0.199475E-03  0.203217E-03   -100.994
   7  -0.525300E-04 -0.270573E-03  0.275625E-03   -100.969
   8  -0.177100E-03 -0.928125E-03  0.944870E-03   -100.786
   9   0.744535E-04  0.390656E-03  0.397688E-03    79.196
  10   0.125331E-03  0.656225E-03  0.668086E-03    79.174
  11   0.167142E-03  0.873862E-03  0.889702E-03    79.158
  12   0.199533E-03  0.104218E-02  0.106110E-02    79.148
  13   0.222429E-03  0.116109E-02  0.118220E-02    79.141
  14   0.235779E-03  0.123047E-02  0.125286E-02    79.139
  15   0.239758E-03  0.125125E-02  0.127401E-02    79.139
  16   0.606309E-04  0.312641E-03  0.318465E-03    79.011
  17  -0.226117E-04 -0.115844E-03  0.118030E-03   -101.027
  18  -0.388141E-04 -0.199473E-03  0.203214E-03   -100.994
  19  -0.525292E-04 -0.270569E-03  0.275621E-03   -100.969
```
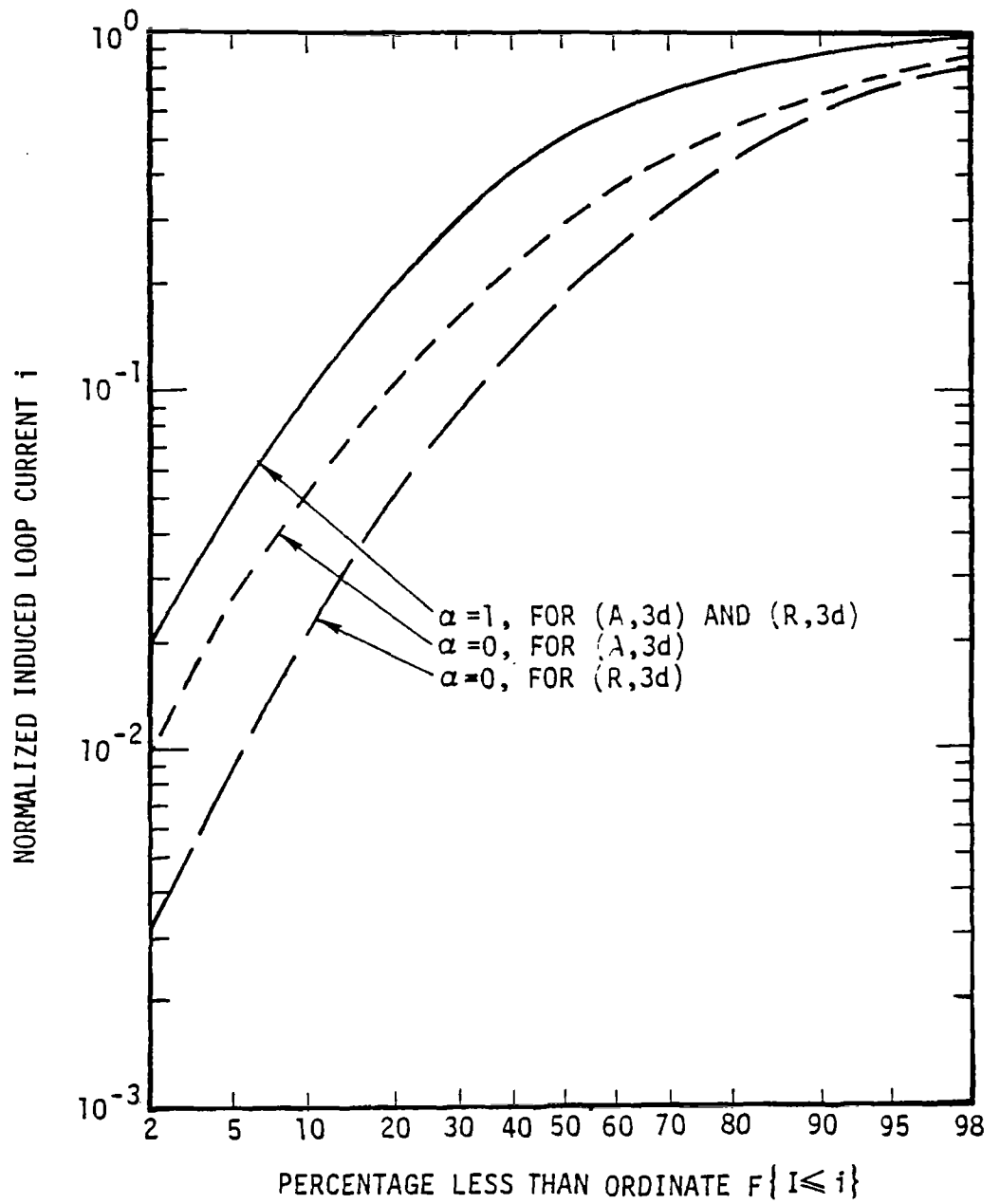
Figure 9   Probability Distribution of the Normalized Induced Loop Currents $I^{(0)}$ for the Three-Dimensional Cases of Equally Probable Area (A,3d) and Equally Probable Radius (R,3d) with Size Parameter $\alpha = 0$, $\alpha = 1$
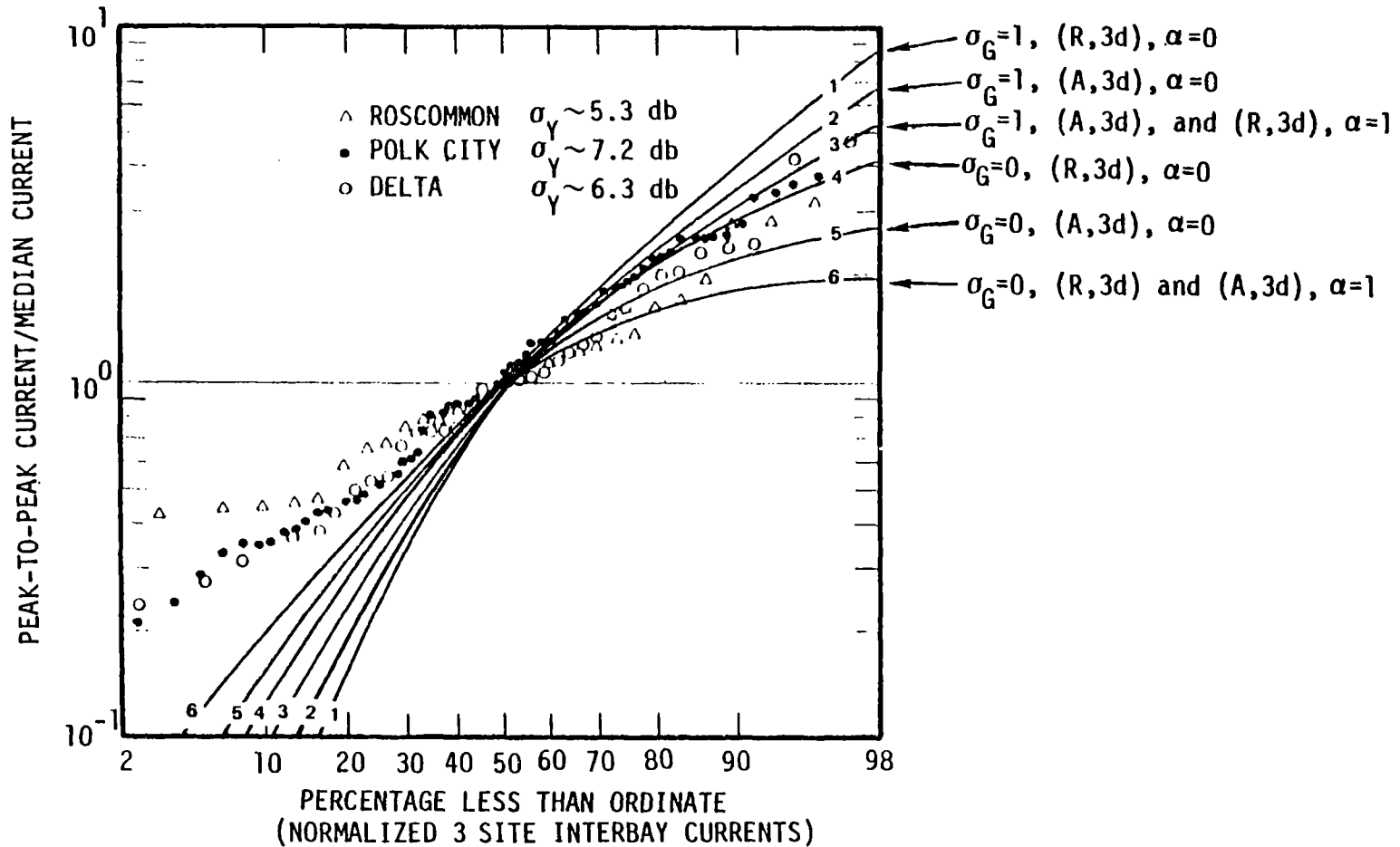
Figure 10. Peak-to-Peak Induced Current Distribution Data for EMP Simulations Obtained in the Program PREMPT and Overlay of 3-D Results

3.3 REMARKS

The results of the model, taken together with the limited available data, lead to the following tentative conclusions. First, our statistical coupling models are not of the type that have a large number of parameters and can be made to fit virtually any data by adjusting these parameters. On the contrary, our models have very few parameters and yield distributions for their major central part insensitive to the values of those few parameters (see Section 3.2 for three-dimensional cases). In view of this, the correspondence between the data and the models, as pointed out in the previous sections, may have important implications in two aspects. On the one hand, the EM coupling to large systems, when dominated by low frequency magnetic fields, is largely <u>insensitive</u> to the coupling detail and yields a distribution whose central part is nearly log-normal with a standard deviation of about 6 dB. On the other hand, precisely because of the insensitivity of the major central part of the distribution to the model, one may not be able to use it to determine the detailed parameters of the coupling (e.g., the loops' orientations, their relative sizes, their mutual coupling strengths, etc.). Second, the shapes of the extreme percentiles of the distribution may depend on and be sensitive to the detailed nature of the coupling. This, combined with the first conclusion, would make apparently plausible assumptions concerning the data distribution function (e.g., log-normal) and the extrapolation to the extreme percentiles based on the central part of the distribution susceptible to substantial errors. Consequently, any conclusions dependent upon such assumptions and extrapolations might be susceptible to substantial errors.

43

REFERENCES AND FOOTNOTES

1. See, e.g., J. R. Mentzer, *Scattering and Diffraction of Radio Waves*, Pergamon Press (1955); F. E. Borgnis and C. H. Papas, *Randwertprobleme Der Mikrowellenphysic*, Sprienger-Verlag (1955).

2. For recent developments in analytical and numerical solutions to such problems, see C. E. Baum (editor), *EMP Interaction Notes*, Air Force Weapons Lab., Albuquerque, N.M.

3. See, e.g., L. D. Landau and E. M. Lipshitz, *Statistical Physics*, Chapter 4 (Addison-Wesley, 1958).

4. A. L. Whitson and E. N. Clark, "AECO AUTOVON Switch Response Similarity," PREMPT Technical Note SRI-20D, July, 1975.

5. See "Summary of Reports Under PREMPT (1305-07 RD Item Report Files PREMPT)" from Harry Diamond Labs. Woodbridge, Virginia (1975) for the description of PREMPT program; also see, e.g., the SRI PREMPT Technical Notes from Stanford Research Institute.

6. The well-known EM properties of small loops and short wires are used freely. See any textbook on EM theory for references, e.g., W. R. Smythe, *Static and Dynamic Electricity* (McGraw-Hill, 1950).

7. For a small loop,

$$\left| \frac{R_{rad}}{\omega L_w} \right| \sim \frac{\sqrt{\frac{\mu}{\varepsilon}}\,(kr)^4}{\omega \mu r} \sim (kr)^3 << 1$$

$$\left| \frac{R_{loss}}{\omega L} \right| \sim \frac{\frac{2\pi r}{\sigma_w 2\pi t \delta_w}}{\omega \mu r} \sim \frac{\delta_w}{2t} << 1$$

where the last inequality uses the assumption that the thickness t of the loop wire is much larger than the conducting loops' skin depth. Using this, (1) implies (2).

8. See any textbook on probability theory, e.g., E. Parzen, Modern Probability Theory and Its Applications, Chapter 7 (Wiley & Sons, 1960).

9. For thin short wires, linear wire current distribution gives $f(M,L) = M/(L/2)$, and $D \ll L$ gives the static self-capacitance

$$C = \frac{\pi \varepsilon L}{4 \ln \left(\frac{L}{D}\right)}$$

Thus

$$\left| \frac{R_{rad}}{\frac{1}{i\omega C}} \right| \sim \left| \frac{\sqrt{\frac{\mu}{\varepsilon}} k^2 L^2}{\frac{1}{i\omega C}} \right| \sim \frac{k^3 L^3}{\ln\left(\frac{L}{D}\right)} \ll 1$$

and

$$\left| \frac{R_{loss}}{\frac{1}{i\omega C}} \right| \sim \left| \frac{\frac{L}{\sigma_w \pi D \delta_w}}{\frac{1}{i\omega C}} \right| \sim \frac{\frac{\delta_w}{D} k^2 L^2}{8 \ln\left(\frac{L}{D}\right)} \ll 1.$$

Again, the last inequality uses the assumption that the wires' diameters, although small compared with the wires' lengths, are not small compared with the conductor's skin depth δ_w at the frequencies considered. Using these, we obtained (6) and (7).

10. W. Feller, An Introduction to Probability Theory and Its Application, Vol. 2, pp. 32 (Wiley & Sons, 1971).

11. This can also be shown formally by using circuit analysis notations. For a linear network, we have for the kth circuit

$$I_k = \frac{V_k}{Z_{kk}} = \frac{V_k^{(0)} + \sum_{j \neq k} I_j \, Z_{jk}}{Z_{kk}} = \frac{\alpha_k E_k + \sum_{j \neq k} I_j \, Z_{jk}}{Z_{kk}}$$

where Z_{kk} is the self-impedance and Z_{ij}, $i \neq j$, are the mutual impedances. Thus, we obtain

$$\sum_j (2Z_{jj} \, \delta_{jk} - Z_{jk}) I_j = \sum_j (\delta_{jk} \, \alpha_j) E_j$$

or in matrix notation

$$\underset{\sim}{Z}' \cdot \underset{\sim}{I} = \underset{\sim}{\alpha} \cdot \underset{\sim}{E}$$

where the matrix $\underset{\sim}{Z}'$ has diagonal elements Z_{ii} and off-diagonal elements Z_{ij}, $i \neq j$. Formally inverting $\underset{\sim}{Z}'$, we get

$$I_k = \frac{\alpha_k E_k}{Z_{kk}} \left\{ 1 + \sum_i Z_{kk} \, \Delta_{ki} \, \frac{\alpha_i E_i}{\alpha_k E_k} \right\} \equiv \frac{\alpha_k E_k}{Z_{kk}} \left\{ 1 + G_k \right\}$$

where

$$\Delta_{ki} \equiv \left[\left(\underset{\sim}{Z}' \right)^{-1} \right]_{ki} - \frac{\delta_{ki}}{Z_{kk}} \xrightarrow[Z_{ij} \to 0]{} 0$$
$$\text{for } i \neq j$$

12. See any probability textbook, e.g., Reference 8, Vol. 1, Chapter 10 (third edition, 1967). Strictly speaking, the fields E_j from all other dipoles $j \neq i$ are not totally independent of each other, because of their mutual couplings. Intuitively, these E_j's are approximately and essentially

independent random variables since their deterministic
mutual coupling mechanisms are controlled by the independent
random variables associated with their geometric
configuration. However, we have not been able to prove
such an approximate and intuitive independence and quantify
rigorously its implication to the applicability of the central
limit theory.

13. Use the integration results

$$\int dx \ln\left[1 + \sqrt{1 - x^2}\right] = \sin^{-1}x + x\left[\ln\left(1 + \sqrt{1 - x^2}\right) - 1\right]$$

$$\int x\,dx \ln\left[1 + \sqrt{1 - x^2}\right] = -V\left[\frac{V\ln V}{2} - \frac{V}{4} - (\ln V - 1)\right]$$

$$\int x^2 dx \ln\left[1 + \sqrt{1 - x^2}\right] = \frac{x^3 \ln V}{3} - \frac{x^3}{9} - \frac{x\sqrt{1 - x^2}}{6} + \frac{\sin^{-1}x}{6}$$

where $V \equiv 1 + \sqrt{1 - x^2}$.

14. See, e.g., J. Aitchson and J. A. Brown, <u>The Log-Normal</u>
    <u>Distribution</u>, The Cambridge University Press (Reprinted
    1963, first printed 1957).

15. The $F\{I^{(o)} \le i\}$ are obtained by integrating the correspond-
    ing densities as:

$$F_{(A,2d)}^{(loop)}\left\{I^{(o)} \le i\right\} = \frac{4}{\pi(i - \alpha^2)}\begin{cases} \int_0^i \sqrt{1 - i^2} - \sqrt{\alpha^2 - i^2}\,di & , \quad 0 \le i \le \alpha \\ \\ \int_0^\alpha di\left(\sqrt{1 - i^2} - \sqrt{\alpha^2 - i^2}\right) \\ \qquad\qquad\qquad\qquad \alpha \le i \le 1 \\ + \int_\alpha^i \sqrt{i - i^2}\,di \end{cases}$$
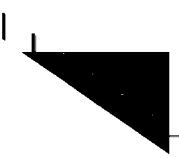
$$= \frac{2}{\pi(1 - \alpha^2)} \begin{cases} i\sqrt{1 - i^2} + \sin^{-1}i - \left(i\sqrt{\alpha^2 - i^2} + \alpha^2 \sin^{-1}\frac{i}{\alpha}\right) , & 0 \le i \le \alpha \\\\ i\sqrt{1 - i^2} + \sin^{-1}i - \alpha^2 \frac{\pi}{2} , & \alpha \le i \le 1 \end{cases}$$

$$F_{(R,2d)}^{(loop)}\left\{I^{(o)} \le i\right\} = \frac{2}{\pi(1 - \alpha)} \begin{cases} \displaystyle\int_0^i \ln\left[\frac{1 + \sqrt{1 - i^2}}{\alpha + \sqrt{\alpha^2 - i^2}}\right] di , & 0 \le i \le \alpha \\\\ \displaystyle\int_0^i di \, \ln\left[1 + \sqrt{1 - i^2}\right] \\\\ \quad - \displaystyle\int_0^\alpha di \, \ln\left[\alpha + \sqrt{\alpha^2 - i^2}\right] \\\\ \quad - \displaystyle\int_0^i di \, \ln i , & \alpha \le i \le 1 \end{cases}$$

$$= \frac{2}{\pi(1 - \alpha)} \begin{cases} \sin^{-1}i - \alpha\sin^{-1}\frac{i}{\alpha} + i \ln\left(\dfrac{1 + \sqrt{1 - i^2}}{\alpha + \sqrt{\alpha^2 - i^2}}\right) , & 0 \le i \le \alpha \\\\ \sin^{-1}i - \dfrac{\pi\alpha}{2} + i \ln\left(\dfrac{1 + \sqrt{1 - i^2}}{i}\right) , & \alpha \le i \le 1 \end{cases}$$

16. See Reference 5.

48

17. See page 9 of Reference 4.

18. See Reference 14.

19. See, e.g., J. A. Stratton, Electromagnetic Theory, p. 279 (McGraw-Hill, 1941).

APPENDIX A
SPECIAL CASES FOR ELECTRIC WIRES

The results of the short electric dipole coupling probability distributions of $I^{(o)}$ for several interesting special cases are given in this section. Here, the notations used are: $K \equiv a^2 \ln b / (b^2 \ln a) \leq 1$; $x_1(i)$ the solution of $x_1^2 \ln b = ib^2 \ln x_1$; and $1 << a \leq L/D \equiv X \leq b$. The analysis follows procedures similar to those in Section 3, but with the basic coupling described by (6) to (10).

A.1 COPLANAR ORIENTATIONS

For the short wires all lying in the $\theta = \pi/2$ plane (see Figure 2) and oriented equally probable in all azimuthal directions, a plane wave incident from the +z axis induces the following current probabilities.

When both wires' lengths X and the relative position of sampled current locations S are fixed, we obtain for the normalized current $I^{(o)}$

$$p_{I^{(o)}(1,2d)}^{(wire)}(i) = \frac{2}{\pi} \frac{1}{\sqrt{1 - i^2}} , \qquad 0 \leq i \leq 1. \qquad (A-1)$$

Here the subscripts (1,2d) indicate the first case considered in two-dimensions. It has a $\mu_{(1,2d)}^{(o)} = 2/\pi = 0.64$ and a $\sigma_{(1,2d)}^{(o)} = (1/2 - 4/\pi^2)^{1/2} = 0.31$.

When X is equally probable in the interval [a,b] and S is fixed, we obtain

$$p_{I^{(o)}}^{(wire)}{}_{(2,2d)}(i) = \frac{2}{\pi(b-a)} \int_{\max(a,x_1(i))}^{b}$$

$$\cdot \, dx \, \frac{b^2 \ln x}{x^2 \ln b \sqrt{1 - \left(\frac{ib^2 \ln x}{x^2 \ln b}\right)}} \, , \qquad 0 \le i \le 1. \tag{A-2}$$

Its average and standard deviation can be obtained numerically.

When X is fixed and the current sampling locations are equally probable anywhere along the wire, S uniform in [0,1], we obtain

$$p_{I^{(o)}}^{(wire)}{}_{(3,2d)}(i) = \frac{2}{\pi} \ln \frac{1 + \sqrt{1 - i^2}}{i} , \qquad 0 \le i \le 1, \tag{A-3}$$

which has a $\mu_{(3,2d)}^{(o)} = 1/\pi = 0.32$ and a $\sigma_{(3,2d)}^{(o)} = (1/6 - 1/\pi^2)^{1/2} = 0.26$.

To investigate the effects of nonnormal incidences, we let the incidence make an angle $\theta_o \ne 0$ with the -z axis. Now the polarization angle Ψ influences the results. For example, if Ψ is a fixed angle ψ_o and both X and S are fixed, then

$$p_{I^{(o)}}^{(wire)}{}_{(4,2d)}(i) = \frac{2}{\pi} \frac{1}{\sqrt{\sin^2 \theta_o' - i^2}} , \qquad 0 \le i \le |\sin \theta_o'|$$

$$\tag{A-4}$$

where θ_o' is the angle between the z axis and the incident polarization $\hat{E}$, $\cos \theta_o' = \cos \psi_o \sin \theta_o$. The (A-4) has a $\mu_{(4,2d)}^{(o)} = \sin \theta_o'/\pi$ and a $\sigma_{(4,2d)}^{(o)} = (1/2 - 4/\pi^2)^{1/2} \sin \theta_o'$. If, instead of a fixed value, the ψ is equally probable in all angles over $[0,2\pi]$, then

$$
p_{I^{(o)}(5,2d)}^{(wire)}(i) = \begin{cases} \displaystyle\int_0^1 f(\xi)\, d\xi & , \; 0 \le i \le \cos \theta_o \\[4mm] \displaystyle\int_{\dfrac{\sqrt{i^2 - \cos^2\theta_o}}{\sin \theta_o}}^1 f(\xi)\, d\xi, & \cos \theta_o \le i \le 1 \end{cases}
$$

(A-5)

where

$$
f(\xi) \equiv \frac{4}{\pi^2} \cdot \frac{1}{(1 - \xi^2)^{1/2} (\xi^2 \sin^2\theta_o + \cos^2\theta_o - i^2)^{1/2}} \cdot
$$

(A-6)

Notice, of course, both (A-5) and (A-6) reduce to (A-1) as $\theta_o \to 0$. The nature of the probability densities (A-1) to (A-5) is depicted by Figure A-1.

A.2 THREE-DIMENSIONAL ORIENTATIONS

For wires with equally probable orientations in a three-dimensional space, the induced currents' probability distributions are independent of the incident and the polarization directions. Except the trivial case of fixed X and fixed S, which incurs a uniform currents' probability distribution,
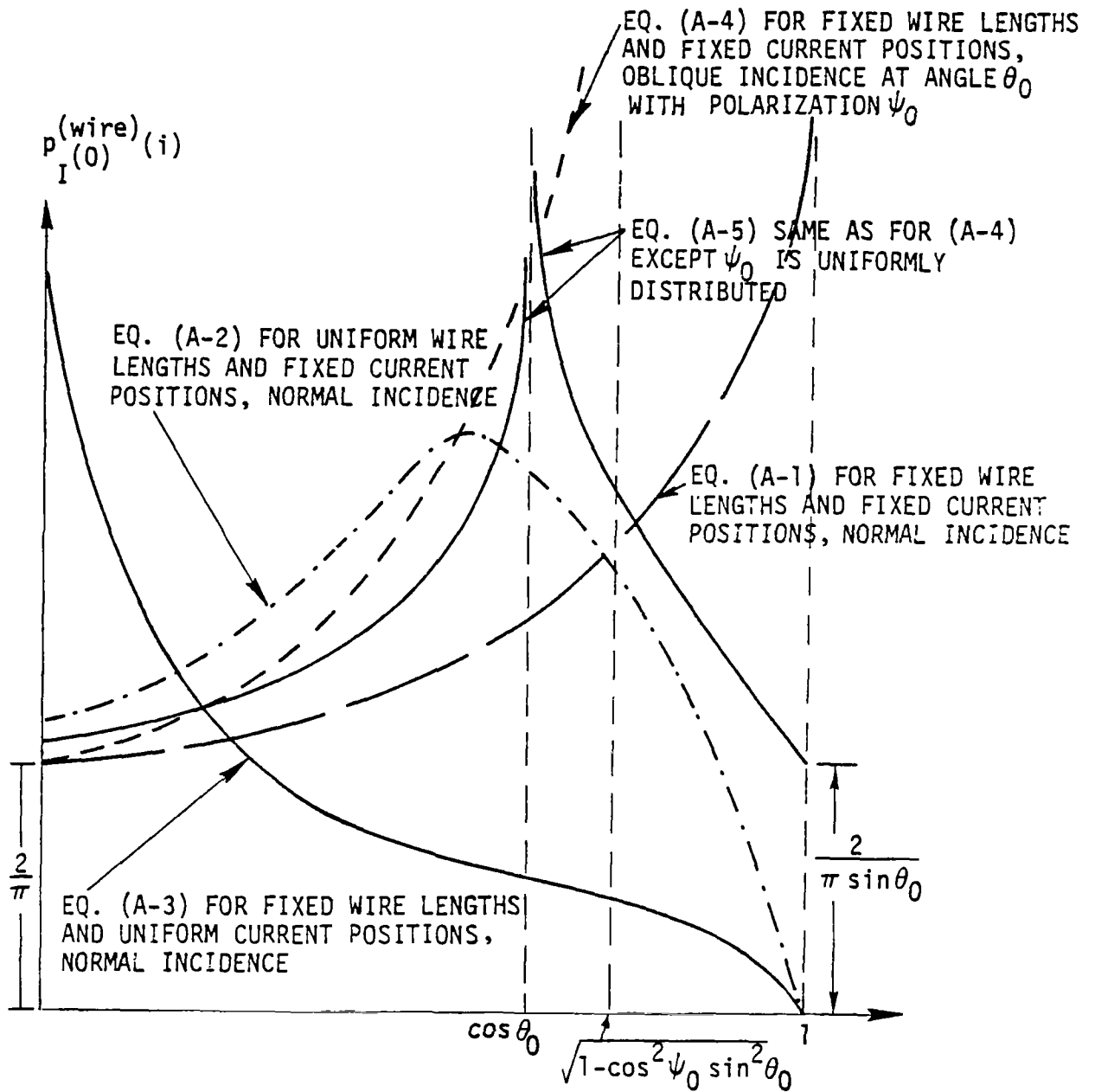
Figure A-1. Probability Densities $P_{I(0)}^{(wire)}(i)$ of Induced Currents on Short Electric Wires Uniformly Oriented in a Plane

several interesting cases are given in the following and their resulting probability densities are sketched in Figure A-2.

If X is uniform in [a,b] and S is fixed, then

$$
p_{I^{(o)}(1,3d)}^{(wire)}(i) = \frac{1}{b-a}
\begin{cases}
\displaystyle\int_a^b dx\, \frac{b^2 \ln x}{x^2 \ln b} \ , & 0 \le i \le K \\[3ex]
\displaystyle\int_{x_1(i)}^b dx\, \frac{b^2 \ln x}{x^2 \ln b} \ , & K \le i \le 1.
\end{cases}
$$

(A-7)

If X is fixed and S is uniform in [0,1], then

$$
p_{I^{(o)}(2,3d)}^{(wire)}(i) = -\ln i, \qquad 0 \le i \le 1 \qquad \text{(A-8)}
$$

which has an average 1/4 and a standard deviation $\sqrt{1/9 - 1/16}$ = 0.22. If both X and S are uniformly distributed, respectively, in [a,b] and [0,1], then

$$
p_{I^{(o)}(3,3d)}^{(wire)}(i) = \frac{b^2}{(b-a)\ln b}
\begin{cases}
\displaystyle -\ln\frac{i}{K} \cdot \int_a^b \frac{\ln x}{x^2}\,dx + \int_K^1 \frac{di'}{i'} \\[2ex]
\qquad \displaystyle \int_{x_1(i')}^b \frac{\ln x}{x^2}\,dx, \ 0 \le i \le k \\[3ex]
\displaystyle \int_i^1 \frac{di'}{i'} \int_{x_1(i')}^b \frac{\ln x}{x^2}\,dx, \qquad K \le i \le 1
\end{cases}
$$

(A-9)
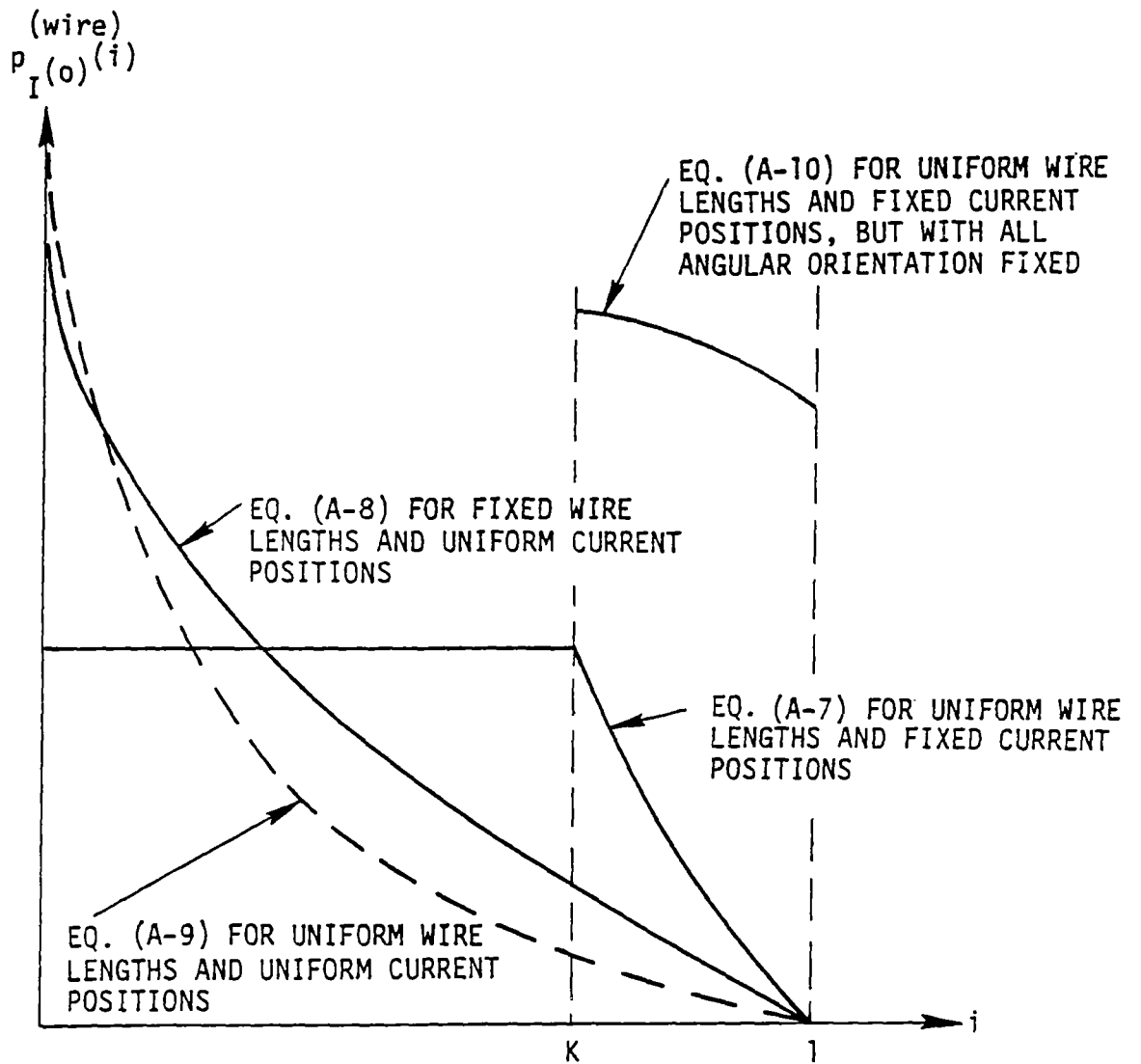
Figure A-2. Probability Densities $p_{I(o)}^{(wire)}(i)$ of Induced Currents on Short Electric Wires Uniformly Oriented in 3-Dimensional Space, Except for Eq. (A-10) which is for all Angular Orientations Being Fixed.

Now, to distinguish the separate effects as caused by the randomness of the lengths X and that of the relative positions S, we consider the wires' orientation, as well as the incident wave direction and polarization, to be fixed. Then, a uniform X in [a,b] and a fixed S gives

$$p_{I^{(o)}(4,3d)}^{(wire)}(i) = \frac{[b\ln x_1(i)]^2}{(b-a) \, x_1(i) \quad \ln b \quad [2\ln x_1(i) - 1]} \, ,$$

$$K \le i \le 1. \qquad \text{(A-10)}$$

However, a fixed X and a uniform S in [0,1] gives simply a uniform $I^{(o)}$ in [0,1], as it should be. Finally, the probability density for both the X uniform in [a,b] and the S uniform in [0,1] is exactly (A-7) again. From these, we clearly see that as far as the induced currents' probability is concerned, the effect of randomness in the current measurement position S, uniform or fixed, is the same as that of randomness in the wire orientations in three-dimensional space.
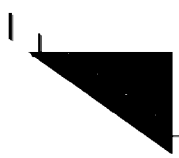
APPENDIX B

ELLIPTICALLY POLARIZED INCIDENCE

If the incident monochromatic EM wave is elliptically polarized, then the coherence of the two superposing perpendicular linear field components substantially changes the nature of the probability density of the basic induced current $I^{(o)}$. To bring out this effect, we shall consider a simple case of an elliptically polarized wave incident upon a short wire of direction $\hat{L}$ from +z axis, with a semi-major axis of polarization in the y-direction and an angle of ellipticity χ in $[0,\pi/4]$ defined by $\left| E_y^{inc}/E_x^{inc} \right| \equiv \tan \chi \leq 1$. Notice that by definition the $\chi \rightarrow 0$ case is a linear polarization, and the $\chi \rightarrow \pi/4$ one is a circular polarization [19]. It follows then that

$$\left| \hat{E} \cdot \hat{L} \right| \equiv \xi = \sin \theta \cdot \sqrt{\cos^2 \phi (1 - \tan^2 \chi) + \tan^2 \chi} \,. \tag{B-1}$$

With this ξ replacing the η in (3) and (6), we obtain the following results.

B.1 COPLANAR ORIENTATIONS

When the wires lie in the $\theta = \pi/2$ plane but orient themselves with equal probability azimuthally and have fixed X and S, we obtain

$$p_{I^{(o)}(1,2d)}^{(wire,\chi)}(i) = \begin{cases} 0 & 0 \leq i \leq \tan \chi \\[2ex] \dfrac{2}{\pi} \cdot \dfrac{i}{\sqrt{1 - i^2}\sqrt{i^2 - \tan^2 \chi}}, & \tan \chi \leq i \leq 1 \end{cases} \tag{B-2}$$

This reduces to (A-1) when $\chi \rightarrow 0$ for a linear polarization, as it should, becomes (i - 1) when $\chi \rightarrow \pi/4$ for a circular polarization which does not distinguish one direction in the plane from another, and has

$$\mu^{(o)}_{\chi(1,2d)} = \frac{2}{\pi} E\left(\frac{\pi}{2}, \sqrt{1 - \tan^2\chi}\right) \qquad \begin{array}{l} \xrightarrow{\chi \rightarrow 0} 2/\pi \\[2mm] \xrightarrow{\chi \rightarrow \pi} 1 \end{array} \qquad \text{(B-3)}$$

$$\sigma^{(o)}_{\chi(1,2d)} = \left\{\frac{\sec^2\chi}{2} - \left[\mu^{(o)}_{\chi(1,2d)}\right]^2\right\}^{1/2} \qquad \begin{array}{l} \xrightarrow{\chi \rightarrow 0} \left(\frac{1}{2} - \frac{4}{\pi}\right)^{1/2} \\[3mm] \xrightarrow{\chi \rightarrow \pi/4} 0 \end{array} \qquad \text{(B-4)}$$

where $E(\phi,k)$ is the elliptical integral of the second kind. Table B-1 shows $\mu^{(o)}_{(\chi,2d)}$ and $\sigma^{(o)}_{(\chi,2d)}$ as functions of χ.

TABLE B-1. AVERAGES AND STANDARD DEVIATIONS FOR INDUCED CURRENT ON WIRES UNIFORMLY ORIENTED IN A PLANE, WITH AN ELLIPTICALLY POLARIZED AND NORMALLY INCIDENT PLANE WAVE

χ (degree)	$\tan \chi$	μ	σ	σ/μ
0	0.0	0.637	0.308	0.483
4.5	0.079	0.643	0.299	0.466
9.0	0.158	0.659	0.280	0.425
13.5	0.240	0.679	0.260	0.382
18.0	0.325	0.707	0.231	0.327
22.5	0.414	0.738	0.203	0.276
27.0	0.510	0.773	0.178	0.230
31.5	0.613	0.818	0.136	0.166
36.0	0.727	0.868	0.100	0.115
40.5	0.854	0.928	0.066	0.071
42.5	0.916	0.959	0.025	0.026
45	1.000	1.000	0	0

B.2 THREE-DIMENSIONAL ORIENTATIONS

When the wires orient equally probable in the three-dimensional space, the probability density for a uniform X in [a,b] and a fixed S is

$$
p^{(wire, X)}_{I^{(o)}(1, 3d)}(i) = \begin{cases} \int_a^b dx \int_{u_o(x)}^{u_1(x)} du & , \ 0 \le i \le K \tan \chi \\[2ex] \int_a^{x_o} dx \int_{u_o(x)}^{1} dx + \int_{x_o}^{b} dx \int_{u_o(x)}^{u_1(x)} du & , \ K \tan \chi \le i \le \min (K, \tan \chi) \\[2ex] \int_a^b dx \int_{u_o(x)}^{1} du & , \ \tan \chi \le i \le K \\[2ex] \int_{x_1}^{x_o} dx \int_{u_o(x)}^{1} du + \int_{x_o}^{b} dx \int_{u_1(x)}^{u_1(x)} du & , \ K \le i \le \tan \chi \\[2ex] \int_{x_1}^{b} dx \int_{u_o(x)}^{1} du & , \ \max (K, \tan \chi) \le i \le 1 \end{cases} \cdot \frac{2i u \left(\dfrac{b^2 \ln x}{x^2 \ln b} \right)^2}{\pi (b-a) \sqrt{1-u^2} [u^2 - u_o^2(x)]^{\frac{1}{2}} [u_o^2(x) - u^2 \tan^2 \chi]^{\frac{1}{2}}} ,
$$

(B-5)

which, of course, reduces to (A-7) as $\chi \to 0$. Here, $u_o(x) \equiv ib^2 \ln x / (x^2 \ln b)$; $u_1(x) \equiv ib^2 \ln x / (\tan \chi \cdot x^2 \ln b)$; $u_o(x_1) \equiv 1$, from which $x_1 \to b$ as $i \to 1$ and $x_1 \to a$ as $i \to K$; and $u_1(x_o) \equiv 1$, from which $x_o \to b$ as $i \to \tan \chi$ and $x_o \to a$ as $i \to K \tan \chi$.

Several special cases of (B-5) are worth noticing. For wires with the same lengths, $a \to b$ and (B-5) reduces to

$$p_{I(o)(3,3d)}^{(wire,\chi)}(i) = \begin{cases} \displaystyle\int_0^1 \\ \displaystyle\int_0^{\sqrt{(1-i^2)/(1-\tan^2\chi)}} \end{cases} d\nu \cdot G(\nu;i,X) \qquad \begin{array}{l} , \ 0 \leq i \leq \tan X \\[3em] , \ \tan\chi \leq i \leq 1 \end{array}$$

$$\text{(B-6)}$$

where

$$G(\nu;i,X) \equiv \frac{2}{\pi} \frac{i}{\sqrt{(1-\nu^2)[1-\nu^2(1-\tan^2\chi)][1-i^2-\nu^2(1-\tan^2\chi)]}} \ .$$

$$\text{(B-7)}$$

This density further reduces to a uniform one as $\chi \to 0$ and to $i/\sqrt{1-i^2}$, with an average $\pi/4 \sim 0.79$ and a $\sigma = (2/3-\pi^2/16)^{1/2} \sim 0.22$, as $\chi \to \pi/4$. In general, the (B-6) starts with value 0 at $i = 0$ and ends with value $(1-\tan^2\chi)^{1/2}$ at $i = 1$.

The general behavior of (B-5) starts with 0 at $i = 0$, reaches a maximum in $0 < i < 1$, and ends with 0 at $i = 1$. Further, as $\chi \to \pi/4$, (B-5) reduces to

$$p_I(i) = \begin{cases} \displaystyle\int_a^b dx \\ \displaystyle\int_{x_1(i)}^b dx \end{cases} \frac{i}{b-a} \cdot \left(\frac{b^2\ln x}{x^2\ln b}\right)^2 \cdot \frac{1}{\sqrt{1-u_o^2(x)}} \qquad \begin{array}{l} , \ 0 \leq i \leq K \\[3em] , \ K \leq i \leq 1 \end{array}$$

$$\text{(B-8)}$$

From the above, we see that for spatially randomly oriented wires with no preferred direction, the elliptically polarized incidence, as compared to a linearly polarized one, makes it less probable for smaller (near zero) induced currents and pushes the most probable current to a higher value (toward the maximum possible current). A basic difference from the linear polarization case is that the probability densities are not a monotonically decreasing function of the induced current amplitude. In view of the similar nature with which the polarizations enter into the basic coupling mechanisms, (1) and (6), these conclusions apply to the magnetic coupling cases as well as to the electric ones.